A Biogeographic Assessment of Seabirds, Deep Sea Corals and Ocean Habitats of the New York Bight: Science to Support Offshore Spatial Planning

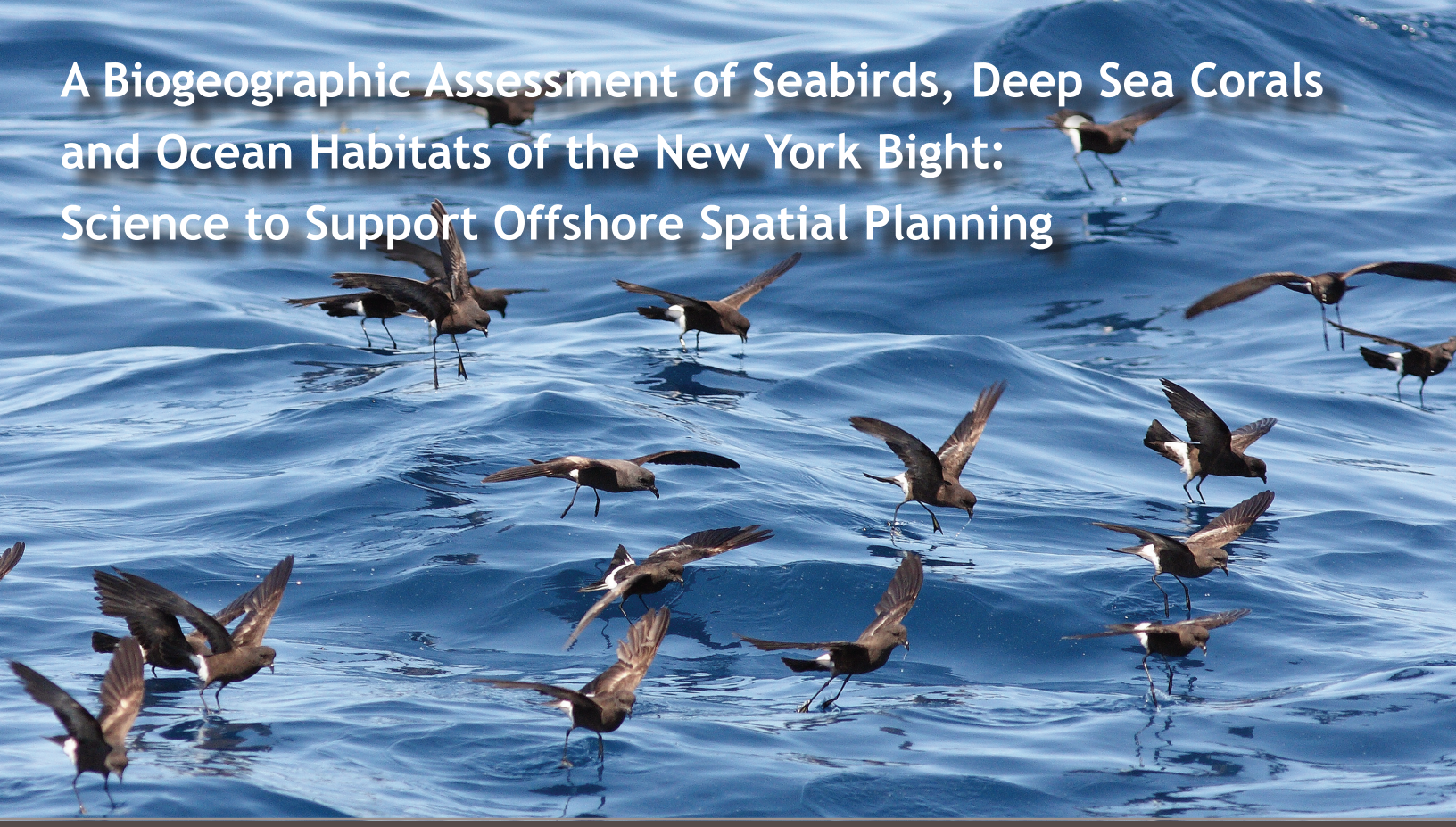

Charles Menza

Brian P. Kinlan

Dan S. Dorfman

Matthew Poti

Chris Caldow

NOAA National Centers for Coastal Ocean Science

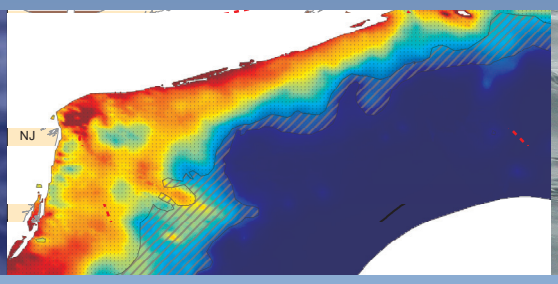

March 2012

NOAA TECHNICAL MEMORANDUM NOS NCCOS 141

NOAA NCCOS Center for Coastal Monitoring and Assessment

Citation

Full report citation:

Menza, C., B.P. Kinlan, D.S. Dorfman, M. Poti and C. Caldow (eds.). 2012. A Biogeographic Assessment of Seabirds, Deep Sea Corals and Ocean Habitats of the New York Bight: Science to Support Offshore Spatial Planning. NOAA Technical Memorandum NOS NCCOS 141. Silver Spring, MD. 224 pp.

Citations for individual chapters (example Chapter 6):

Kinlan, B.P., C. Menza, and F. Huettmann. 2012. Chapter 6: Predictive Modeling of Seabird Distribution Patterns in the New York Bight. pp. 57-127. In: C. Menza, B.P. Kinlan, D.S. Dorfman, M. Poti and C. Caldow (eds.). A Biogeographic Assessment of Seabirds, Deep Sea Corals and Ocean Habitats of the New York Bight: Science to Support Offshore Spatial Planning. NOAA Technical Memorandum NOS NCCOS 141. Silver Spring, MD. 224 pp.

Acknowledgments

This work would not have been possible without the numerous contributors who shared their data, time and expertise. Many people are acknowledged among the individual chapters of this report, but we must also thank Jamie Higgins for organizing and formatting the content of this report, as well as Kevin McMahon, Sarah Hile, Tom McGrath and Moe Nelson for preparing this report for publication.

Cover and Back

Seabird photos on the front and back cover were provided by D. Pereksta (BOEM); the wind turbine photo on the front cover was provided by A. Meskens (Wikimedia Commons); the coral *Madrepora occulata* on the front cover was provided by Islands in the Sea 2002, NOAA/OAR; the large photo of the coral *Paragorgia hirez* on the back cover was provided by MBRI/NOAA and the small photo of the sponge by Mountains in the Sea Research Team, IFE/NOAA; and the gray seafloor map was provided by US Geogological Survey.

A Biogeographic Assessment of Seabirds, Deep Sea Corals and Ocean Habitats of the New York Bight: Science to Support Offshore Spatial Planning

Prepared by the
Biogeography Branch (BB)
Center for Coastal Monitoring and Assessment (CCMA)
National Centers for Coastal Ocean Science (NCCOS)
National Oceanic and Atmospheric Association National Ocean Service (NOAA)
1305 East West Highway (SSMC-IV, N/SCI-1)
Silver Spring, MD 20910
USA

March 2012

Editors

Charles Menza
NOAA Center for Coastal Monitoring and Assessment
Biogeography Branch

Brian P. Kinlan
NOAA Center for Coastal Monitoring and Assessment, Biogeography Branch and
Consolidated Safety Services, Inc., Fairfax, VA, under NOAA Contract No. DG133C07NC0616

Dan S. Dorfman
NOAA Center for Coastal Monitoring and Assessment, Biogeography Branch and
Consolidated Safety Services, Inc., Fairfax, VA, under NOAA Contract No. DG133C07NC0616

Matthew Poti
NOAA Center for Coastal Monitoring and Assessment, Biogeography Branch and
Consolidated Safety Services, Inc., Fairfax, VA, under NOAA Contract No. DG133C07NC0616

Chris Caldow
NOAA Center for Coastal Monitoring and Assessment
Biogeography Branch

NOAA Technical Memorandum NOS NCCOS 141

United States Department of Commerce

John Bryson
Secretary

National Oceanic and Atmospheric Administration

Jane Lubchenco
Administrator

National Ocean Service

David Kennedy
Assistant Administrator

This page intentionally left blank.

About this document

This report provides a compilation of maps and spatial assessments of bathymetry, surficial sediments, oceanographic habitat variables, deep sea corals, and seabirds for offshore waters of New York. The information was compiled to support an offshore spatial plan being developed by the New York Department of State's Ocean and Great Lakes Program (OGLP). The report is a product of collaboration started in 2009 between scientists at the National Oceanic and Atmospheric Administration's National Centers for Coastal Ocean Science (NCCOS) and coastal managers at OGLP. NCCOS and OLGP worked closely to identify priority scientific needs, plan the analytical approach, assess existing data, and compile findings into this report. The targeted users of this report are coastal managers at OGLP, but other State and federal decision-makers, offshore renewable energy development interests and environmental advocates will also find the information useful.

The presented data and maps are the most accurate and up-to-date ecological information available for the study area. The diverse ecological themes which are treated here represent priority data gaps and were requested by OGLP to better understand and balance ocean uses and environmental conservation. The data will feed into a larger project led by OGLP to compile and assess existing data for offshore spatial planning.

NCCOS is a recognized scientific leader in developing biogeographic assessments. These assessments are organized around the development of geospatial data layers for ecological parameters, integrated analyses, and specific quantitative products to aid in resource management. The spatial analyses in this report build on and advance existing biogeographic techniques developed by NCCOS for other coastal and marine areas, including the Gulf of Maine, North and Central California, and the Northwestern Hawaiian Islands. This report, along with similar biogeographic products from around the nation, is also available online. For more information please visit NCCOS' webpage (http://coastalscience.noaa.gov/) or direct questions and comments to:

Chris Caldow
Biogeography Branch Chief
National Oceanic and Atmospheric Administration /National Ocean Service/National Centers for Coastal Ocean Science/Center for Coastal Monitoring and Assessment/Biogeography Branch
Phone: (301) 713-3028 x164
E-mail: Chris.Caldow@noaa.gov

Or

Jeff Herter
Offshore Spatial Planning Research and Development Manager
Ocean and Great Lakes Program
New York Department of State
Phone: (518) 408 - 4799
E-mail: jeff.herter@dos.state.ny.us

Table of Contents

Chapter 6: Appendices 149

Chapter 6: Online Supplements

Online Supplements can be found by going to http://oceanservice.noaa.gov/programs/nccos/welcome.html and searching on the keywords: *New York Spatial Plan*

Online Supplement 6.1: Predictor variable transformation details
This document provides additional detail on the statistical preparation of potential predictor variables for analysis.

Online Supplement 6.2: Species and group seasonal models, full diagnostic reports
This Online Supplement is presented in the form of an HTML document providing links to full diagnostic reports from each of the seasonal species/group predictive models.

Executive Summary

This report provides a compilation of new maps and spatial assessments for seabirds, bathymetry, surficial sediments, deep sea corals, and oceanographic habitats in support of offshore spatial planning led by the New York Department of State Ocean and Great Lakes Program. These diverse ecological themes represent priority information gaps left by past assessments and were requested by New York to better understand and balance ocean uses and environmental conservation in the Atlantic. The main goal of this report is to translate raw ecological, geomorphological and oceanographic data into maps and assessments that can be easily used and understood by coastal managers involved in offshore spatial planning.

*Image 0.1. Roseate Tern (*Sterna dougallii*) in flight. This species is endangered in the Mid-Atlantic. Photo credit: David Pereksta, BOEM.*

New York plans to integrate information in this report with other ecological, geophysical and human use data to obtain a broad perspective on the ocean environment, human uses and their interactions. New York will then use this information in an ecosystem-based framework to coordinate and support decisions balancing competing demands in their offshore environment, and ultimately develop a series of amendments to New York's federally approved Coastal Management Program.

The targeted users of this report and the compiled spatial information are New York coastal managers, but other State and federal decision-makers, offshore renewable energy development interests and environmental advocates will also find the information useful. In addition, the data and approaches will be useful to regional spatial planning initiatives set up by the Mid-Atlantic Regional Council on the Ocean (MARCO) and federal regional planning bodies for coastal and marine spatial planning.

This report represents a synthesis of existing information rather than a new data collection effort. Given the short time frame over which management decisions frequently need to be made and the high cost of new natural resource surveys, this approach may be one other coastal zone managers will want to consider. The data and maps were developed by employing a spatial analytical approach which applies predictive modeling and geostatistics to interpolate among data, identify important spatial patterns and develop continuous distribution maps of species and physical resources at fine spatial resolutions required to support spatial management decisions. This analytical approach also allows for a quantitative description of prediction certainty a useful parameter for spatial planning. For example, maps of prediction reliability can be used to target efforts to collect new survey data to fill information gaps, or to incorporate measures of certainty into risk assessments.

In Chapter 2, a new bathymetric model with spatially-explicit certainty estimates is presented which builds on previous predictive bathymetric modeling approaches in the region. The new model provides a continuous gridded bathymetric surface for the study area, and allows users to view and explore spatial variation in the vertical accuracy of depth predictions. The new model is similar to the National Oceanic and Atmospheric Administration's Coastal Relief Model but provides estimates of prediction certainty, which can be used to prioritize locations for new bathymetric surveys and better understand the reliability of depth predictions and derived spatial layers (e.g., benthic habitats, positions of depth contours).

Predictive models of mean grain size, sediment composition, and hard bottom occurrence were developed to map the distribution of surficial sediments and habitats on the seafloor. These new models presented in

Chapter 3 build upon the data compilations and analytical frameworks laid out by existing work in the area. For mean grain size and sediment composition (e.g., mud, sand, gravel) the models provide continuous, gridded spatially-explicit prediction surfaces and corresponding certainty estimates. A hard bottom occurrence model also provides a continuous gridded prediction surface representing the likelihood of hard bottom habitats.

In Chapter 5, the locations of deep sea coral and sponge records within NOAA's Deep Sea Coral Research and Technology Program's geodatabase are examined within the New York Bight. Predictive models were not developed for deep sea corals or sponges because of limitations on the quantity and type of data available within the New York Study area. Instead, we focused on mapping known locations of deep sea corals and sponges, discussing their role as important habitat for other marine organisms, and discussing and summarizing past studies in the region.

In Chapter 6, new maps of the seasonal and annual distributions of seabird species and seabird ecological groups are provided. These distributions were predicted based on statistical models fit to visual shipboard seabird observational data collected as part of a standardized survey program from 1980-1988. Species and group distributional models were then combined to produce "hotspot" maps depicting multi-species abundance and diversity patterns. Spatial predictors included long-term archival satellite, oceanographic, hydrographic, and biological datasets. Seabird distributional maps for seasonal and annual relative indices of occurrence and abundance were produced, accompanied by maps depicting metrics of certainty. The resolution of predictions is approximately 400 times finer than previous 10 arc-minute maps of seabird distribution in this region. These high-resolution, contiguous predictive maps of seabird distribution are expected to be useful contributions to offshore spatial planning, particularly of activities that may affect seabirds or their habitats.

Introduction

Charles Menza[1], Chris Caldow[1], Jeff Herter[2], and Greg Capobianco[2]

1.1. A CALL FOR SPATIAL PLANNING OFFSHORE OF NEW YORK

New York depends on healthy coastal and marine ecosystems for its thriving economy and vibrant communities. These ecosystems support critical habitats for wildlife and a growing number of significant and often competing ocean uses and activities, such as fishing, commercial transportation, recreational boating and energy production. Planners, policy makers and resource managers are being challenged to sustainably balance ocean uses and environmental conservation in a finite space and with limited information. Solutions to these challenges are complicated by emerging industries, climate change, and a growing coastal population with shifting needs.

Image 1.1. Offshore wind farm.
Photo credit: A. Meskens (Wikimedia Commons)

New York is addressing competition and evolving threats to coastal and marine resources and services by compiling spatial information and applying ecosystem-based management to spatial planning. In 2006, the New York Oceans and Great Lakes Ecosystem Conservation Act created the New York Oceans and Great Lakes Ecosystem Conservation Council and charged the New York Department of State (DOS) with developing amendments to its federally-approved Coastal Management Program to better manage human activities that impact coastal and marine ecosystems.

The Coastal Management Program within DOS has broad authority to guide human uses and can use the consistency determination process, outlined in the Coastal Zone Management Act of 1972 (Public Law 92-583, 16 U.S.C. 1451-1456), to affect decisions made in both federal and state waters. Ultimately amendments will be integrated into state and federal permitting processes related to siting ocean uses and regional ocean planning programs. A state with an approved Coastal Management Program has the authority to approve or deny a proposed federal action if it may affect the state's coastal resources.

DOS is taking a phased approach for developing amendments by focusing on the most pressing issues first. New York's first amendment will apply to the Atlantic waters off New York out to the continental shelf and will focus on guiding decisions for new clean, renewable energy production and transmission, while addressing conflicts with other human activities and protecting critical habitats. Future amendments will include Long Island Sound and the Great Lakes.

New York has joined a growing number of states and federal agencies thinking about offshore spatial planning. For instance, Massachusetts and Rhode Island have recently completed ocean management plans, and New Jersey, Oregon and California are in the process of developing plans or collecting information necessary for planning purposes. In addition to state-level planning initiatives, multi-state partnerships and the federal government are undertaking spatial planning and have adopted a regional approach. The regional approach was chosen to allow for the variability of economic, environmental, and social aspects among different areas, provide an ecosystem-based perspective, and match existing regional governance structures.

[1] Center for Coastal Monitoring and Assessment, National Centers for Coastal Ocean Science, National Ocean Service, National Oceanic and Atmospheric Administration
[2] Ocean and Great Lakes Program, New York Department of State

In 2009, the governors of New York, New Jersey, Delaware, Maryland and Virginia committed to a comprehensive regional approach to address challenges faced in the ocean waters of the Mid-Atlantic, and created the Mid-Atlantic Regional Council on the Ocean (MARCO). The council has since developed action teams to protect critical habitats, improve water quality, support sustainable development of renewable energy, prepare for climate change, and build capacity for effective spatial planning in the region. Many of the data and analytical approaches used in this report will likely be useful to the entire mid-Atlantic region.

The MARCO initiative fits in well with the first ever National Ocean Policy signed by President Obama in 2010 (Executive Order 13547, 2010). The policy seeks to improve stewardship of the oceans, coasts, and Great Lakes by way of: adopting ecosystem-based management; obtaining, advancing, using, and sharing the best science and data; promoting efficiency and collaboration; and strengthening regional efforts. The order established the National Ocean Council to guide implementation of the policy, and identified nine national priority objectives, one of which is to implement coastal and marine spatial planning (CMSP). The Council outlined a flexible framework for spatial planning that is regional in scope, developed cooperatively among federal, state, tribal, and local authorities, and includes substantial stakeholder, scientific, and public input (NOC, 2012).

According to U.S. Executive Order 13547, CMSP is a "comprehensive, adaptive, integrated, ecosystem-based, and transparent spatial planning process, based on sound science, for analyzing current and anticipated uses….[CMSP] identifies areas most suitable for various types or classes of activities in order to reduce conflicts among uses, reduce environmental impacts, facilitate compatible uses, and preserve critical ecosystem services to meet economic, environmental, security, and social objectives."

1.2. DATA TO SUPPORT OFFSHORE SPATIAL PLANNING

New York requires accurate, accessible and integrated ecological and human use data in order to base spatial planning on sound science. Whenever possible, these data are needed at spatial and temporal scales that are in line with management decisions, and need to provide continuous information over the whole management domain. With these requirements in mind, over the past year New York has compiled diverse ecological and human use datasets, including: biogeographic data from The Nature Conservancy's Northwest Atlantic Marine EcoRegional Assessment (NAMERA); distributions of marine fishes, marine mammals and sea turtles from Stone Environmental Inc., the University of Rhode Island, the New England Aquarium, and the National Marine Fisheries Services' Northeast Fisheries Science Center; infrastructure data, chiefly from the NOAA electronic navigation charts; jurisdictional information downloaded from the Multi-purpose Marine Cadastre (MMC), a tool developed in collaboration between NOAA Coastal Services Center (CSC) and DOI's Bureau of Ocean Energy Management (BOEM – formerly the Bureau of Ocean Energy Management, Regulation and Enforcement, BOEMRE), and; offshore human use information collected through participatory geographic information system workshops developed and carried out in partnership between the New York State Coastal Management Program and CSC.

This report supplements other datasets and reports compiled by OMAFRA's Great Lakes Program (OGLP), and provides data identified by OGLP as a priority to satisfy the needs of a Coastal Management Program amendment in the Atlantic. Specifically, this report examines the spatial distribution of: seabirds, bathymetry, surficial sediments, deep sea corals, and dynamic oceanographic habitats. We developed new geospatial synthesis products with the objective of providing:

- The most accurate and up-to-date information available,
- Continuous information over the management domain and at the finest spatial scale raw data would support,
- Estimates of synthesis product reliability (certainty) and assessments of data quality,
- Data products in digital formats that allow easy integration with other datasets in a geographic information system, and
- Maps, assessments and interpretations that are easily understood and used by coastal managers to support spatial management decisions.

All data and assessments in this report represent a synthesis of existing information rather than a new data collection effort. Given the short time frame over which management decisions frequently need to be made and omnipresent budget constraints, this approach of interest to be one other coastal zone managers.

1.3. AN ANALYTICAL APPROACH USEFUL TO SPATIAL PLANNING

The ocean area offshore of New York has a significant amount of raw data, ranging from sediment samples to bird observations to ocean temperature profiles. But many of these datasets are spatially and temporally limited or exist only as scattered points. As such, they are difficult to use for spatial planning, especially when decisions must be made in locations that are in-between surveys, have few surveys, have widely varying measurements or require a regional context. Where possible, we overcame these challenges by using a spatial analytical approach which applied statistical modeling to generalize from scattered sets of data points to regional maps of important patterns and processes.

Not all data can support this type of spatial analytical approach, especially datasets with few observations and/or with unknown sampling effort. For instance, predictive coral and sponge distribution models could not be developed in this report (Chapter 5) due to these data limitations. In this case, the goal was not to make spatial predictions, but rather to compile the most up-to-date observations and develop maps providing the best available information to make management decisions.

In the remaining chapters, datasets for bathymetry (Chapter 2), surficial sediments (Chapter 3), dynamic oceanographic habitats (Chapter 4), and seabirds (Chapter 6) included sufficient information to develop reliable spatial models. In-depth discussions of the statistical methods used to convert observation point data into continuous surfaces are available in corresponding chapters. A generalized representation of the approach using actual data (common loon sightings) is presented in Figure 1.1.

The spatial analytical approach follows Cressie (1993) and Hengl et al. (2007), where the variables of interest are modeled as a linear combination of components representing a deterministic mean trend, a spatially structured random process, and non-spatially structured error. The deterministic mean trend is estimated using a suitable broad spatial-scale function (generalized linear model for seabirds, or a smoothing function for bathymetry and surficial sediments) and the spatially structured random process and error term are estimated by geostatistical analysis of the residuals. There is no loss of information in this approach since the residuals contain all of the information removed from the trend surface.

The result is a spatially-explicit distribution of predicted outcomes, whether the outcomes are of abundance or the likelihood of occurrence. This predicted distribution of outcomes has two uses. First, the average taken from of the distribution can be mapped and used to represent the most likely outcome for a given location. Second, the distribution provides an estimate of certainty for the mapped outcome. That is, the mapped prediction for an area with a narrow distribution (outcomes are similar) has greater certainty, than the prediction for an area with a wide distribution (outcomes are dissimilar). Knowledge of a prediction's certainty is a useful measure in spatial planning, because it allows planners to use the best available data to make decisions with an understanding of limitations on generalizations that can be made from the available data. We use the terms reliability, certainty and uncertainty throughout this report.

The applied spatial predictive methods involve a number of statistical assumptions, and it is important to note that the accuracy of model predictions and estimates of certainty depend to varying degrees on these assumptions being met. A complete discourse on all statistical assumptions is beyond the scope of this report (for detailed discussions see the methodological citations in each of the individual analytical chapters of this report), but several general assumptions are:

- *Spatial patterns and sampling effort are constant over the analyzed timeframe*

  To compile sufficient data to make predictions we integrated data over several years. This approach provides information on the long-term average state of the system, but ignores long-term trends or cycles.

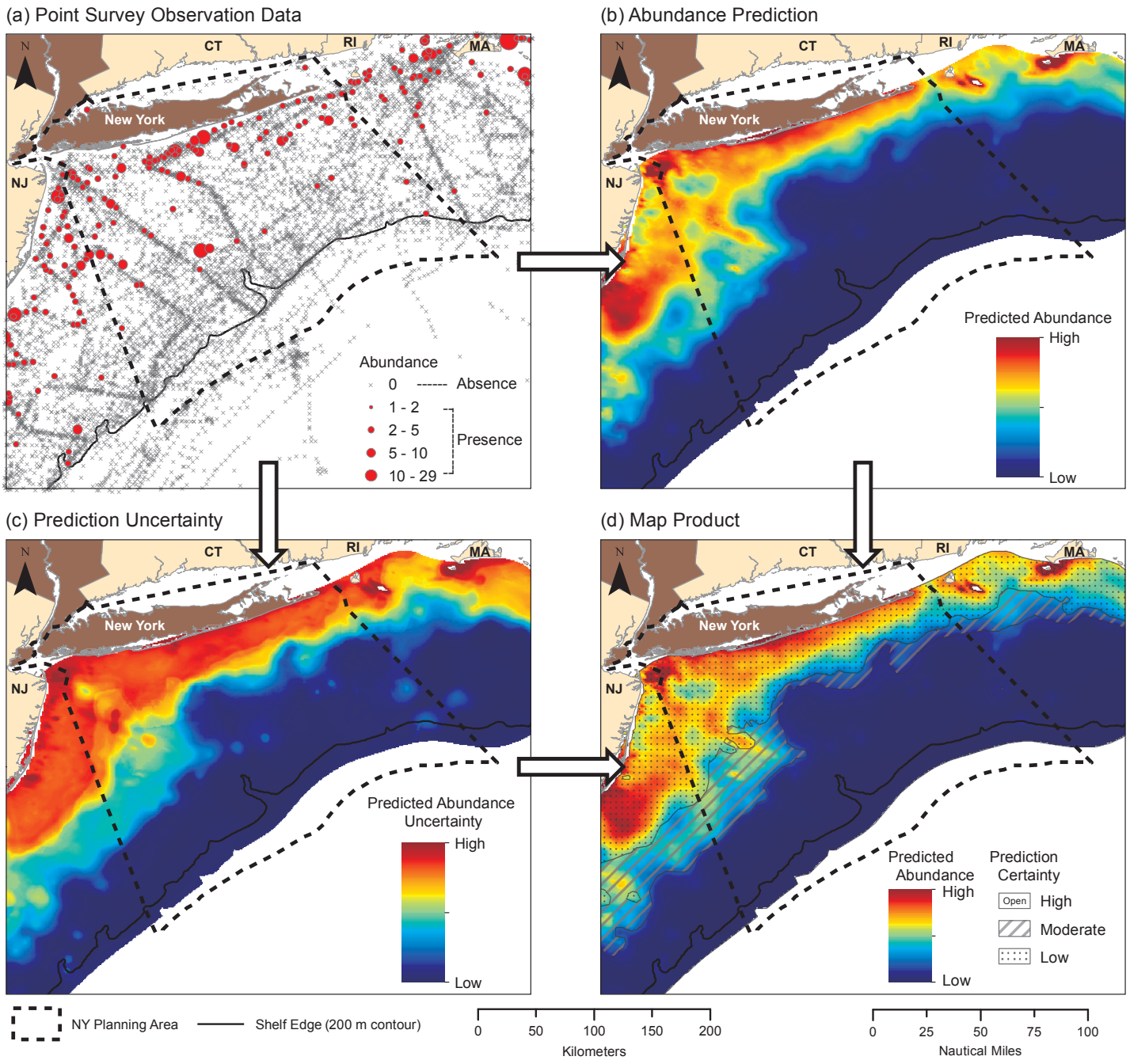

Figure 1.1: These four panels show the general analytical approach used in this report to develop continuous distribution maps, assess certainty, and make easily understood products from typical survey data. This example uses data from the Manomet Bird Observatory Seabird and Cetacean Assessment Program database. Panel A shows common loon sightings distributed across the study area. A clear spatial pattern is difficult to discern, since sampling effort is irregular and observed presences are dispersed among observed absences. This is a typical ecological pattern since seabirds move around, detection is not perfect and sampling effort is irregular. Panel B shows the continuous output from a predictive model which has linked observations of the common loon to environmental predictors such as sea surface temperature, depth and oceanographic productivity. The model displays the average likelihood of observing a common loon given these environmental linkages and fills in gaps where survey data is missing. Panel C displays the uncertainty related to the predictive model, where areas of most uncertainty indicate the greatest range in possible predicted outcomes. Model uncertainty is commonly greatest where the resource of interest is most variable or where few data are available. Panel D shows a map where certainty (the inverse of uncertainty) is draped over predicted relative abundance. This type of map was requested by coastal resource managers in OGLP, because it was easy to understand and use for spatial management decisions.

- *Resources and species are precisely detected and measured*

Species or resources are seldom perfectly detectable, meaning corresponding occurrence and abundance estimates will be biased compared to true abundance and occurrence values. When sampling effort is known and heterogeneous, values can be standardized by effort to allow relative comparisons, but difficulties still arise in assessing areas where little sampling effort was devoted.

- *There exists a constant relationship between sampling effort, relative indices of occurrence and abundance, and true values of occurrence and abundance*

Not only are species and resources unlikely to be perfectly detectable, the relationship between relative indices of occurrence and abundance and the true values of occurrence and abundance could vary in time and space, depending on differences in observers, weather conditions, animal behavior, etc. Such variation introduces an unaccounted for source of measurement error into data, and it is not possible to correct for all such sources of variation.

In addition to the assumptions inherent in modeling techniques, maps and assessments are a reflection of data quality and we assume that the data quality is suitable for spatial modeling and are representative of the ecosystem's true state. The key challenges of using existing data are that it was collected for a specific purpose, which may not be congruent with spatial analysis, and by definition it was collected in the past. It is important to understand potential limitations inherent to each dataset, and in each chapter we have identified and assessed key data quality issues.

We understand that statistical and data quality assumptions may not be completely met, thus model validation is an important part of the modeling approach. Validation is usually done by cross-validation, a process in which some data are left out of model fitting and model predictions are tested against those data. Model predictions can also be tested against high-precision "ground-truth" datasets where such datasets are available. We use both methods to validate predictions and maps in this report.

1.4. DESCRIPTION OF THE STUDY AREA

This report focuses on a study area in ocean waters off the coast of New York. The area covers a portion of the Mid-Atlantic Bight and much of the area characterized as the New York Bight. The study boundaries extend from the southern shores of Long Island to the edge of the continental shelf and from Nantucket Shoals to the shores of New Jersey (Figure 1.2). Both state and federal waters are included.

The study area covers a "spatial planning area" chosen by the OGLP in which they will focus their planning efforts, as well as ocean waters immediately adjacent to the planning area. The spatial planning area includes New York's territorial sea and Federal waters where natural phenomena and human activities can affect services and resources within the territorial sea.

The majority of the study area is characterized by a broad continental shelf approximately 150-200 km wide. At its outer edge, the shelf meets the continental slope, an area 40-60 km wide with very steep slopes and that extend to depths greater than 2 km. The most prominent topographic features in the study are the Hudson shelf valley, which crosses the entire shelf, and several shelf edge incisions made by submarine canyons. These topographic features alter the broad-scale hydrography of the region, are important to cross-shelf water movement and provide important benthic habitats which differ from the surrounding seascape (Cooper, 1987; Steimle et al., 1999).

The seafloor on the shelf is composed of mostly sand which grades to silt and clay in deeper areas (Poppe et al., 2005). The relatively homogenous seafloor has sporadic relic sand and gravel ridges; exposed sandstone and bedrock, dumping sites, dredge disposal sites and artificial reefs (i.e., shipwrecks, lost cargo, submerged pipelines). Bottom sediments play critical roles as habitats for benthic organisms such as demersal fish, clams and corals, and in storage and processing of settling organic matter.

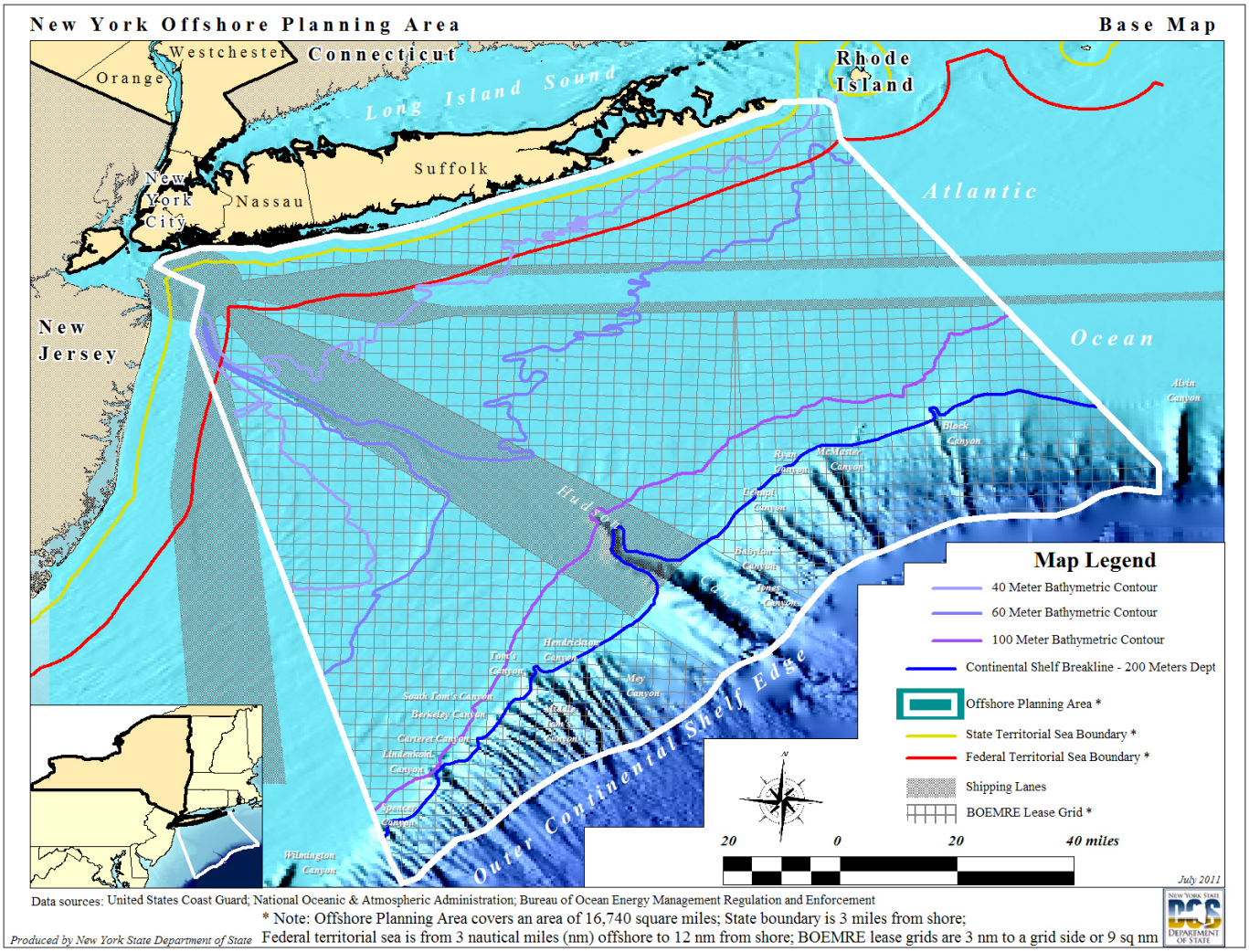

Figure 1.2: A map of the study area used in this report. Map produced by New York State Department of State. Note that, effective October 1, 2001, the Bureau of Ocean Energy Management, Regulation and Enforcement (BOEMRE) was renamed to the Bureau of Ocean Energy Management (BOEM).

The hydrography of the study area is characterized by a strong seasonal cycle, considerable freshwater input from rivers, storm dominated sediment transport and interactions among large distinct water masses which extend across the Northwest Atlantic (Townsend et al., 2006). These hydrographic characteristics, along with characteristics of the seafloor and geomorphological setting produce patterns across multiple spatial and temporal scales in resources (e.g., fish, sand, renewable energy) and ecosystem services (e.g., coastal protection, tourism and transportation).

1.5. REFERENCES

Cooper, R.A., P. Valentine, J.R. Uzmann, and R.A. Slater. 1987. Submarine canyons. In R.H. Backus and D.W. Bourne. eds. Georges Bank. p. 52-65. MIT Press, Cambridge, MA.

Cressie, N.A.C. 1993. Statistics for spatial data (revised ed.). New York: John Wiley & Sons, Inc.

Executive Order 13547. 2010. Stewardship of the ocean, our coasts, and the great lakes. President Barack Obama, Office of the Press Secretary. July 19, 2010.

Hengl, T., G.M.B. Heuvelink, and D.G. Rossiter. 2007. About regression-kriging: from equations to case studies. Computers and Geosciences, 33(10):1301-1315.

NOC (National Ocean Council). 2012. Draft National Ocean Policy Implementation Plan. http://www.whitehouse.gov/administration/eop/oceans/implementationplan. Plan released January 12, 2012. Website accessed February 20, 2012.

Poppe, L.J., S.J. Williams, and V.F. Paskevich. 2005. U.S. Geological Survey East-Coast Sediment Analysis: Procedures, Database, and GIS Data: Open-File Report 2005-1001, U.S. Geological Survey, Coastal and Marine Geology Program, Woods Hole Science Center, Woods Hole, MA.

Steimle, F.W. C.A. Zetlin, P.L. Berrien, D.L. Johnson, and S. Chang. 1999. Tilefish (*Lopholatilus chamaeleonticeps*) life history and habitat characteristics. U.S. Department of Commerce, NOAA Technical Memorandum NMFS-NE-152, 30 p.

Townsend, D.W., A.C. Thomas, L.M. Mayer, M. Thomas, and J. Quinlan. 2006. Oceanography of the Northwest Atlantic Continental Shelf. pp. 119-168. In: Robinson, A.R. and K.H. Brink (eds). The Sea, Volume 14, Harvard University Press.

This page intentionally left blank.

Bathymetry

Matthew Poti[1,2], Brian Kinlan[1,2,3], and Charles Menza[1]

2.1 SUMMARY

A new bathymetric model with spatially-explicit uncertainty estimates was developed for the New York study area (Figure 1.1). The model builds on previous predictive bathymetric modeling approaches in the region (e.g., Calder, 2006), provides a continuous gridded bathymetric surface for the study area, and allows users to view and explore spatial variation in the vertical accuracy of depth predictions. The spatial resolution of the model is identical to the National Oceanic and Atmospheric Administration's (NOAA) Coastal Relief Model (CRM; horizontal resolution approximately 83.8 m) in the study area and was built from the same database of hydrographic survey points. Unlike the CRM, the new geostatistical model provides estimates of prediction certainty, which can be used to prioritize locations for new bathymetric surveys and better understand the reliability of depth predictions and derived spatial layers (e.g., benthic habitats, positions of depth contours).

2.2 BACKGROUND

Bathymetry (also called seafloor topography) is an important base environmental layer for spatial planning since it influences both planning of human activities (e.g., construction, shipping) and many physical, chemical and ecological processes. For instance, reliable bathymetric information can simultaneously improve habitat conservation and energy development by supporting the identification of:

- Unique or vulnerable benthic habitats
- Distributions of rare or endangered species
- Efficient corridors for transmission lines
- Suitable sites for turbine platforms, and
- Potential construction hazards

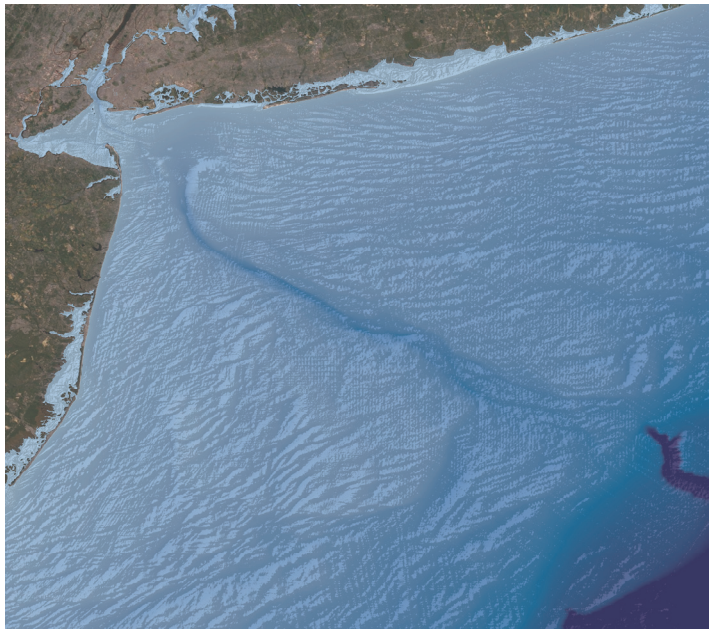

Image 2.1. An example of a bathymetric surface in the New York Bight, showing the change in depth with distance from shore and the complexity of the seafloor across the shelf. The Hudson Shelf Valley is prominently visible in the center of the model as the area of darker blue extending from New York harbor (top left) towards the shelf edge (bottom right). Coastal managers and engineers use bathymetric surfaces to assess shipping lanes, identify fish habitats, lay undersea cables and find sand and gravel resources. The bathymetric surface shown here is the the NOAA Coastal Relief Model (CRM), draped over a derived hillshade layer to highlight bathymetric variation. Terrestrial imagery is the ArcGIS Online World User Imagery layer (ESRI Online).

Bathymetry can be measured by a range of instruments, which determine the precision, spatial resolution, extent and cost of bathymetric information and nautical charts. Until the latter half of the 20th century, lead lines dropped from a ship were used to estimate depths (Calder, 2006) and were compiled on charts to give a coarse-scale representation of the seafloor and identify navigation hazards. Lead lines were eventually replaced by more accurate vertical beam echosounders (VBES) and subsequently by multibeam echosounders (MBES). Modern MBES can collect millions of precise soundings efficiently and quickly, making possible high-resolution bathymetric maps that reveal fine-scale features of the seafloor (Calder, 2006). Horizontal positioning technologies have also advanced over the years from sextant-based navigation to modern GPS.

When combined with backscatter information and validation samples, MBES data offers an unprecedented view of the composition and morphology of the seafloor at multiple spatial scales (Kostylev et al., 2001; Gardner et al., 2003). The States of Oregon and California recently collected new data to take advantage of insights

[1] Center for Coastal Monitoring and Assessment, National Centers for Coastal Ocean Science, National Ocean Service, National Oceanic and Atmospheric Administration
[2] Consolidated Safety Services, Inc., under NOAA Contract No. DG133C07NC0616
[3] Corresponding author: Brian.Kinlan@noaa.gov

provided by MBES and these data have been integrated into state spatial planning initiatives, specifically the Oregon Territorial Sea Plan and California Marine Life Protection Act Initiative. On the East Coast, fewer states have comprehensive MBES coverage; this may be a reflection of the increased costs involved in surveying comparatively wide, shallow continental shelves.

About 20% of the New York planning area is covered by MBES surveys (Figure 2.1) which have been collected by the United States Geological Survey (USGS), NOAA and the Woods Hole Oceanographic Institution (Schwab et al., 1997a and 1997b; Butman et al., 1998; Goff et al., 1999; Butman et al., 2006). The corresponding data have helped researchers map benthic habitats and identify physical features on the seafloor within the footprints of surveys.

Unfortunately, the incomplete distribution of multibeam surveys limits their usefulness for understanding the relative distribution of habitats, features, processes and species over the entire planning area, a critical component of integrated marine spatial planning. The U.S. Coastal Relief Model developed by the National Geophysical Data Center (NGDC; http://www.ngdc.noaa.gov/mgg/coastal/model.html) offers a 3-arc second continuous bathymetric model that covers the majority of the study area (including all of the continental shelf and slope). The CRM is derived from the largest single compilation of bathymetric soundings for US coastal waters and has been used effectively to inform spatial planning on the East Coast as part of the Massachusetts

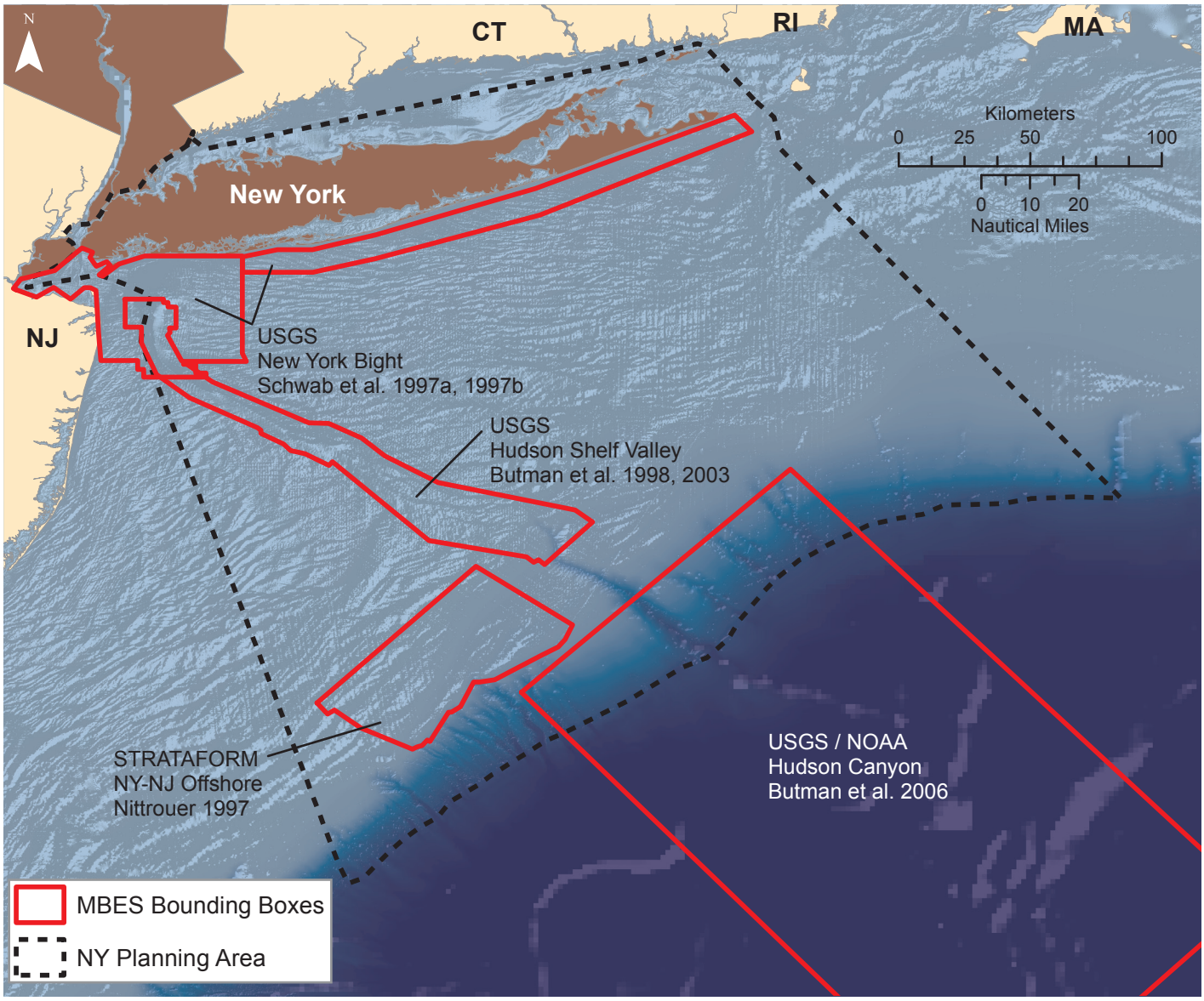

Figure 2.1. Spatial extent of selected multibeam and sidescan sonar surveys in the study area. Survey boundaries are overlaid on bathymetry data from the Coastal Relief Model blended with the ETOPO1 Global Relief Model (Amante and Eakins 2009).

Ocean Plan and Rhode Island Special Area Management Plan. Although coarser than multibeam data, the ~84 m horizontal resolution of the CRM is still sufficient to resolve general features of interest for marine spatial planning (e.g., canyons, ridges, sand waves, bathymetric contours).

The portion of the CRM that overlaps the New York planning area was produced in 1999 and is a compilation of historical hydrographic surveys, collected using VBES and MBES from various data sources, including NOAA, USGS, the U.S. Army Corps of Engineers, and various academic institutions. Although compiled surveys are brought together under a common spatial framework, they possess different spatial footprints and resolutions, and were collected using different instruments. Newer surveys commonly overlap, adjoin and supersede older surveys.

Generally, the CRM is used in resource management applications assuming the depth measurements and predictions to be accurate, but significant uncertainty in model depth estimates arises from measurement error in hydrographic surveys, methods used to interpolate between survey points and data processing (discussed in detail in Calder, 2006 and references therein). These errors are variable over the study area (Figure 2.2) due to various factors, including survey age, processing guidelines, and distances amongst soundings. Since bathymetric errors in the CRM are not quantified, users cannot know whether depth predictions at a given location are likely to deviate from the true value by a few centimeters or hundreds of meters. Disregarding uncertainty might be acceptable for some analyses conducted at coarse spatial resolutions, but is problematic for finer resolution analyses and when precise measurements are needed. Knowing where bathymetric predictions are precise and where they are not provides managers with information to define and manage risk associated with decisions relying on bathymetry or derived products (e.g., defining benthic habitats, estimating construction costs, placing shipping lanes).

2.3 METHODS

2.3.1 General Modeling Approach

A geostatistical modeling approach was used to predict a continuous, gridded bathymetric surface from scattered sounding points and to generate corresponding spatially-explicit uncertainty estimates. Geostatistical methods are based on the premise that neighboring samples are more similar than samples farther away (Tobler, 1970), a phenomenon known as spatial autocorrelation. Spatial autocorrelation can be detected, quantified and modeled by semivariogram analysis, and used to make predictions at locations that have not been measured

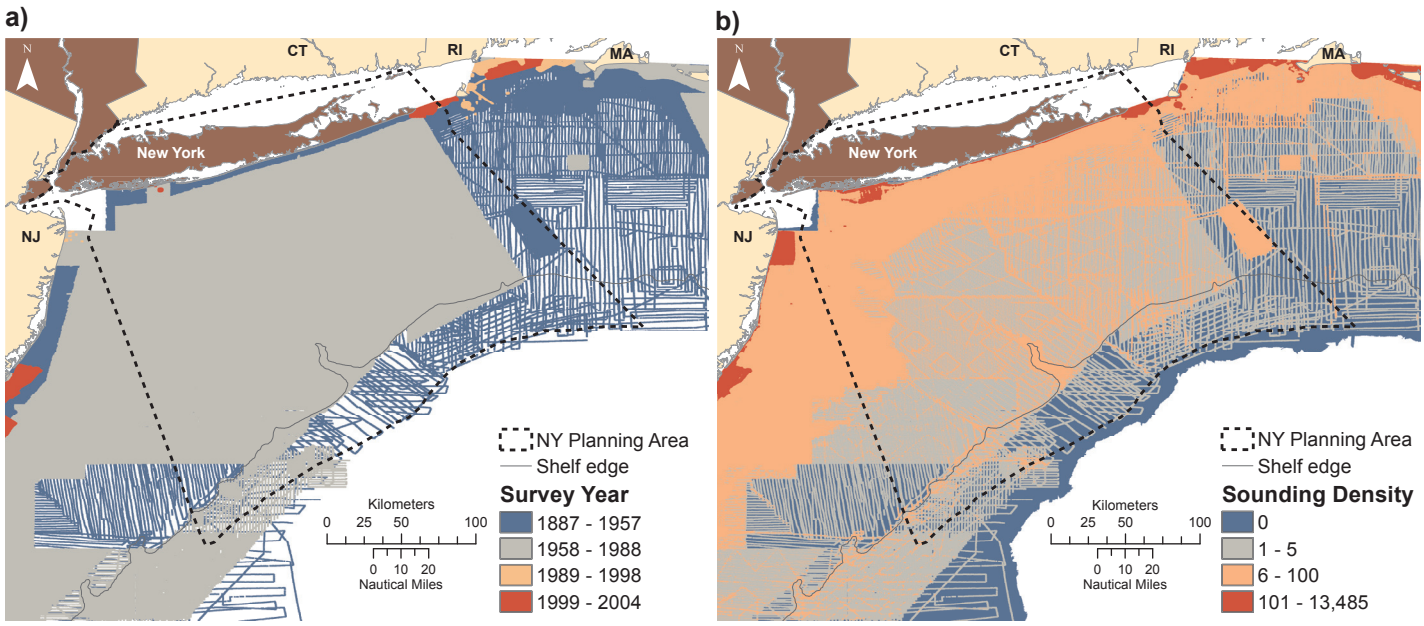

Figure 2.2. (a) Most recent survey year for soundings within 1 km rectangular neighborhoods. Survey year classes generally correspond with the evolution of horizontal positioning and vertical sounding technologies. More recent soundings tend to be more precise. (b) The number of bathymetric soundings per square kilometer. The shelf edge corresponds to the 200 m depth contour.

(Cressie, 1993; Chiles and Delfiner, 1999). In addition, the same spatial model used to develop predictions can be used to model uncertainty (i.e., expected precision) of predictions.

The geostatistical modeling approach used here follows Cressie (1993), where estimates of depth for a given location, Z(x,y), are modeled as a linear combination (sum) of components representing a deterministic mean trend, μ(x,y), a spatially structured random process, δ(x,y), and non-spatially structured error, ε.

$$Z(x,y) = \mu(x,y) + \delta(x,y) + \varepsilon \qquad \text{(Equation 2.1)}$$

Equation 2.1 defines the workflow used to arrive at Z(x,y). The deterministic mean trend and spatially structured random process with error term are modeled separately and then combined by summation (see Figure 2.3 for schematic representation of work flow). The deterministic mean trend, μ(x,y), is estimated using a suitable smoothing function and residuals of original data from this smoothing function are computed at the data positions by subtracting the trend prediction from the observed data value. The spatially structured random process, δ(x,y), and error term, ε, are then estimated by fitting a suitable semivariogram model to the empirical semivariogram of the residuals. The error term is defined by the semivariogram nugget and represents error that is not spatially correlated, which includes both measurement error and variability occurring at spatial scales shorter than the sampling resolution (Cressie, 1993).

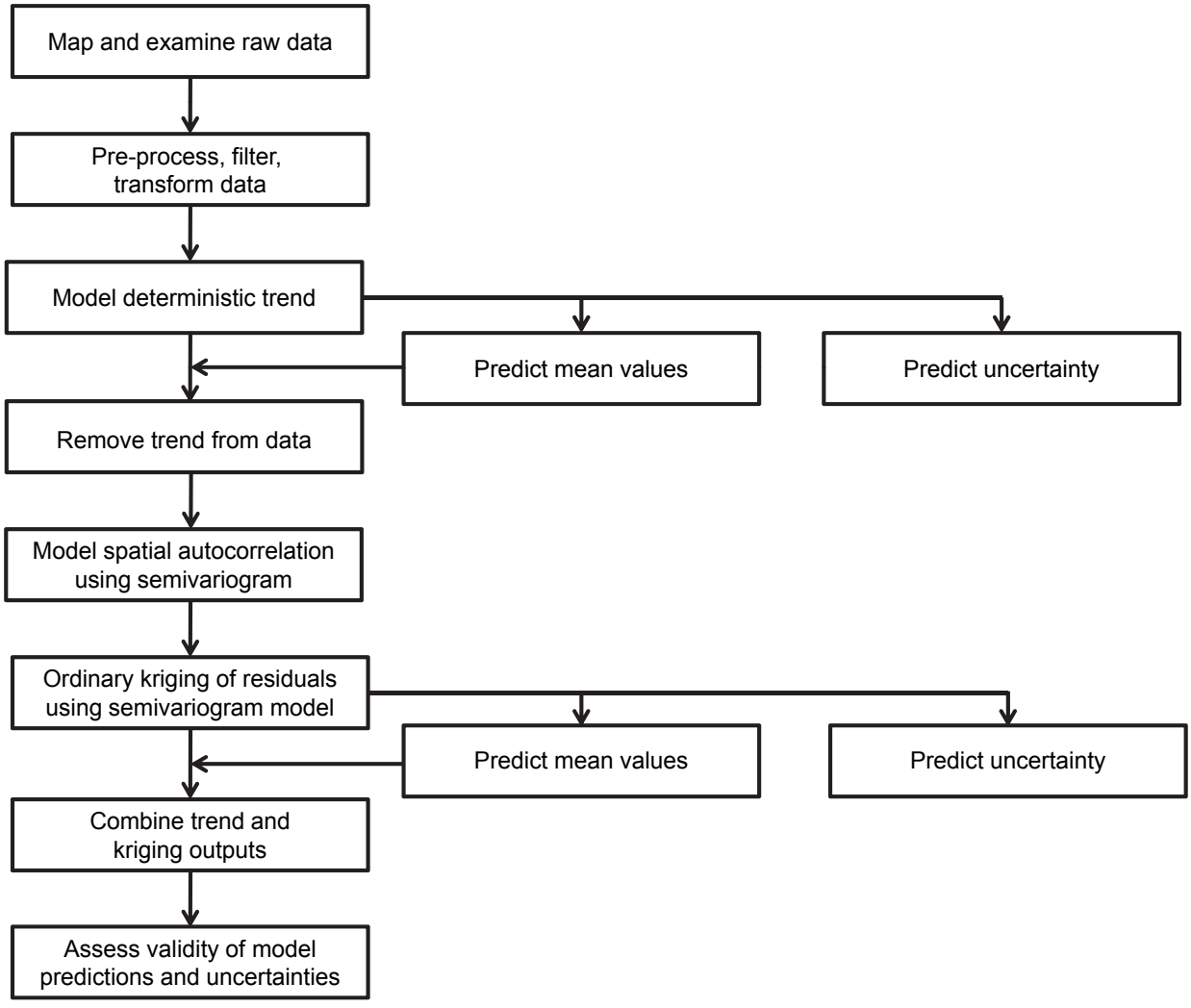

Figure 2.3. General workflow describing the geostatistical approach used to develop the predictive model for bathymetry (see sections 2.3.3 and 2.3.4 for a more detailed description of the methods).

Geostatistical models involve a number of statistical assumptions (for detailed discussions see Cressie, 1993; Chiles and Delfiner, 1999). The accuracy of model predictions and uncertainty bounds depends to varying degrees on these assumptions being met. Thus, an important part of any geostatistical analysis is model validation, which is usually done by cross-validation, a process in which some data are left out for purposes of model fitting and model predictions are tested against those data. Model predictions can also be tested against high-precision "ground-truth" datasets where such datasets are available. We use both methods to validate model predictions in this chapter (see Section 2.3.4).

2.3.2 Data Acquisition and Preparation

Raw Sounding Data

To develop a new geostatistical bathymetric model for the NY Bight, all available National Ocean Science (NOS) Hydrographic Survey Data overlapping the study area were downloaded from the National Geophysical Data Center Hydrographic Survey Database (http://www.ngdc.noaa.gov/mgg/bathymetry/hydro.html) on April 21, 2011. Survey measurements and metadata were extracted from raw HYD93 formatted files and exported into plain ASCII text tabular files using custom parsing scripts. Depths are represented as positive numbers with increasing depth below sea level defined by the Mean Lower Low Water (MLLW) vertical datum. Sounding data were merged with survey metadata, so that information detailing when and how each sounding was collected was retained. Sounding locations, originally in decimal degrees (NAD83 datum), were projected into a Universal Transverse Mercator projection (UTM 18N), since subsequent processing requires measurement of point-to-point distances in a Cartesian coordinate system. UTM 18N has its central meridian at 75ºW and thus allows calculation of distances in our study area with negligible distortion relative to grid resolution (83.8 m).

Hydrographic soundings in the study area come from a multitude of surveys distributed between 1887 and 2004. Surveys used an assortment of positioning and sounding technologies, resulting in a patchwork of overlapping soundings collected with variable sample spacing and different precisions (Figure 2.2). In addition, survey data was processed using varying methods which created varying post-processing errors (see Calder, 2006 for a full discussion). These errors can propagate to the final model creating distortions that do not correspond to changes on the seafloor. While steps have been taken to partially correct for and reduce the impact of these data quality issues, it is important to understand that they cannot be entirely eliminated. No bathymetric model based on historical hydrographic sounding data will be completely free from such considerations.

In general, the vast majority of soundings were retained to maximize data density. However, some soundings were corrected or eliminated prior to modeling. First, based on Calder (2006), we applied a +1.48 m correction to all soundings collected by lead line to correct for the observed bias of lead line soundings compared to multibeam sonar measurements. Second, lead line and VBES surveys were identified that showed evidence of quantization due to rounding to the nearest whole fathom (resulting in an error of up to 1.8 m). Data from these surveys were eliminated when they were located within the footprint of more accurate surveys (i.e., surveys that did not exhibit quantization). Survey footprints were hand digitized at 1:50,000 in ArcGIS 10 (ESRI, 2011). Different types of rounding and conversions created surveys with varying degrees of quantization, but only those surveys with the most severe fathom-rounding quantization of 1.8 m were eliminated from analysis, and those only when more recent information was present. Other types of quantization are expected to result in errors less than 1 m. Other sources of error in raw soundings, including un-accounted for changes in vertical and tidal datums, are expected to be small (on the order of 10's of centimeters) and are discussed in detail in Calder (2006).

Depth Stratification

The resulting hydrographic sounding database was divided into four strata based on depth thresholds (Table 2.1). Thresholds were chosen based on depth ranges that correspond to different maximum uncertainty specifications under International Hydrographic Organization (IHO) standards (S.44 Order 1 and 2, IHO 1998) and on coarse-scale changes in geomorphology (e.g., the continental shelf break). Neighboring strata overlap slightly to facilitate merging of outputs from individual strata into a continuous surface.

Table 2.1. Depths used to stratify hydrographic soundings and the corresponding number of soundings within each stratum.

DEPTH STRATUM	NUMBER OF SOUNDINGS (EXCLUDING OVERLAP)	PERCENTAGE OF SOUNDINGS	ADDITIONAL SOUNDINGS FROM OVERLAP	PERCENTAGE OF SOUNDINGS FROM OVERLAP
0-30 m	2,077,055	83.9%	0	0%
30-100 m	337,238	13.6%	176,843	34.4%
100-200 m	21,932	0.9%	9,931	31.2%
200-2,000 m	40,196	1.6%	3,517	8.0%
Total	2,476,421	100%	190,291	7.1%

Transformation

Prior to statistical modeling, depth values were transformed using the following logarithmic function to normalize error distributions:

$$Z_{transform} = \log(Z*b+a) \qquad \text{(Equation 2.2)}$$

where Z is depth in meters (with positive numbers representing depth below sea surface) and the transformation parameters a and b are taken from the appropriate error model for each depth stratum identified by IHO standards (a = 0.5 m, b = 0.013 when Z < 100 m [IHO S.44 Order 1] and a = 1.0 m, b = 0.023 when Z >= 100 m [IHO S.44 Order 2]) (IHO, 1998). This transformation was based on a standard bathymetric error model formulation (IHO, 1998; Calder, 2006), and improves homogeneity of conditional error variances within local regression and kriging neighborhoods, a desirable statistical property.

2.3.3 Development of the Bathymetric Model

The deterministic mean bathymetric trend surface was estimated using LOESS, a semi-parametric local regression technique (Cleveland and Devlin, 1988). LOESS estimates a smooth trend surface using weighted least-squares regression in local neighborhoods defined by a fixed number of points closest to each prediction location (the span, measured as a percentage of the total number of data points). Specifically, quadratic LOESS was used with a span of 1%, corresponding to an average neighborhood width of between 3 and 12 km depending on point density.

LOESS was implemented in Matlab version 7.13 (R2011b) with the Curve Fitting toolbox (The MathWorks Inc., Natick, MA). The standard Matlab toolbox function (curvefit/curvefit/+curvefit/LowessFit.m) was modified to reduce processing times and increase matrix stability. Execution speed was improved by using k-dimensional search trees (KD-Tree for MATLAB, Tagliasacchi, 2011) to identify and sort soundings in each local neighborhood. Under certain conditions local regression methods such as LOESS can exhibit instability due to limits on the precision of matrix calculations. X and Y coordinates were centered and re-scaled to minimize the possibility of matrix stability problems. The condition number of each local regression design matrix was also evaluated to diagnose areas where matrix precision might affect the accuracy of regression fits.

Local regression matrix stability was problematic when points that were very close to each other had very different values, which occasionally occurred in areas of high sounding density and resulted in gaps in the LOESS prediction surface. To eliminate gaps, soundings within a horizontal distance of ± 10 cm were identified, grouped and then dispersed with a small random nudge. Coordinates for the first occurrence of a sounding in a group were retained and subsequent coordinates were shifted by adding a uniform random number in the range ± (0.5,1.5 m). Displacements were only accepted if they did not create conflicts (within 10 cm) with other soundings. A total of 700 soundings were modified (<0.03% of all data). Although this dispersion adds some positional error to each sounding, the displacement is negligible in relation to other sources of positioning error caused by geographic positioning systems or ship heave/pitch/roll.

A similar displacement procedure was applied to soundings that fell within 10 cm of the prediction grid coordinates. The purpose of this was to ensure that measurement and micro-scale error were filtered out of the prediction surface, because at the precise locations of original data, the kriging prediction surface exhibits

spikes due to the nugget effect. Filtering the nugget effect in this way is similar to the maximum *a posteriori* resampling technique proposed for filtering noisy bathymetric data by Goff et al. (2006).

The parametric standard error of the mean trend was estimated using a Monte Carlo approach. Specifically, the approximation method of Durban, et al. (1999) was used to estimate the variance-covariance matrix of the estimated local regression coefficients, $Var(\hat{\beta})$. The scale of the variance-covariance matrix was estimated as the sum of squares of the residuals for the whole model (i.e., the residuals of the original data from the LOESS fit at all data points), divided by (N – λ), where N is the number of observations and λ is the effective number of parameters, estimated as, λ = 2*(1+[N/(N*span)]).

Regression coefficient vectors were simulated by 1,000 draws from a multivariate normal distribution defined by mean vector $\hat{\beta}$ and covariance matrix $Var(\hat{\beta})$, and the LOESS prediction was re-calculated for each simulated regression coefficient vector. The standard error was estimated as the standard deviation of the simulated LOESS predictions at each location. The condition number of the design matrix of each local regression was also recorded as an additional diagnostic measure.

Residuals were obtained by subtracting the LOESS trend surface prediction at each data location from the observed data value. Semivariograms of residuals were then calculated and modeled in ArcGIS 10 with the Geostatistical Analyst extension (ESRI, 2011). A separate anisotropic semivariogram model was fit independently for each depth stratum (Figure 2.4, Table 2.2). The nugget effect was adjusted manually based on visual inspection and prior expectations from measurement error models (see below). The rest of the model parameters, including anisotropy ranges and direction, were fit automatically using non-linear weighted least-squares (ESRI, 2011).

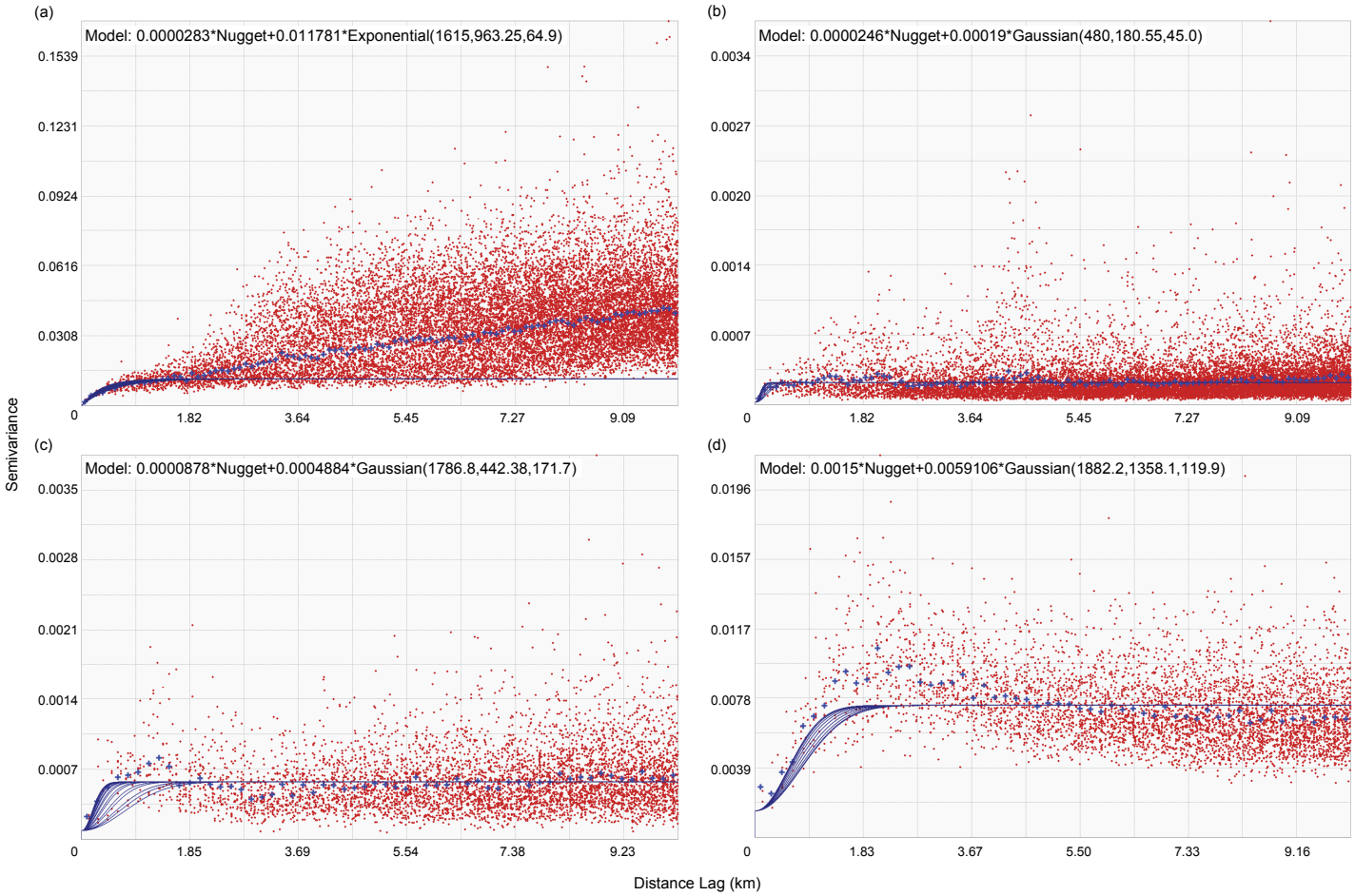

Figure 2.4. Estimated semivariograms of residuals and fitted semivariogram models for each depth stratum. (a) 0-30 m, (b) 30-100 m, (c) 100-200 m, (d) 200-2,000 m. Red dots represent sample semivariance values, blue crosses represent averaged semivariance values, solid blue lines represent directional semivariogram model fits.

Table 2.2. Semivariogram parameters for each depth stratum.

DEPTH STRATUM (m)	n	TYPE OF VARIO-GRAM MODEL	NO. OF LAGS	LAG SIZE (m)	NUGGET $x10^{-5}$(m)	MAJOR RANGE (m)	MINOR RANGE (m)	DIREC-TION (°)*	PARTIAL SILL $x10^{-3}$	% OF THE SILL DUE TO THE NUGGET
0-30	2,077,055	Exp	100	100	2.83	1,615	963.25	64.86	11.8	0.2
30-100	514,081	Gau	100	100	2.46	480	180.55	45.00	0.19	11.5
100-200	31,863	Gau	175	58	8.78	1,787	442.38	171.74	0.488	15.2
200-2,000	43,713	Gau	180	56	150.0	1,882	1,358.12	119.88	5.91	20.2

Exp= exponential; Gau= Gaussian; *Clockwise from North

Nugget selection was guided by a Monte Carlo simulation of measurement error expected for each depth stratum based on maximum measurement error models defined by IHO standards (IHO S.44 Orders 1 and 2). We simulated depth observations with measurement error across the depth range of each stratum (n=100,000 points), log-transformed the simulated depths using Equation 2.2, calculated residuals from the recorded depth, and calculated the depth-averaged measurement error for each stratum in the log-transformed space. This served as a lower bound on the nugget for semivariogram fitting, which was then adjusted higher if necessary based on the best fit to empirical semivariogram plots. The rationale for this approach is that the minimum value of the nugget is equal to measurement error. Small-scale spatial features not resolved by the sample spacing (so-called "micro-scale structures") can add to this error and raise the value of the nugget, but not lower it.

To perform ordinary kriging of residuals, semivariogram model parameters fitted in ArcGIS 10 (ESRI, 2011) were input into the KT3D module of GSLIB (Geostatistical Software Library, Deutsch and Journel, 1992). KT3D was used instead of ArcGIS 10 because of the prohibitively slow computational speed of the ArcGIS kriging implementation. KT3D was run with ordinary kriging, 8-sector search neighborhoods, a minimum search radius necessary for a gap-free kriging prediction, and a maximum search radius equal to the minimum radius times the anisotropy ratio. At least 1 and no more than 80 points (a maximum of 10 from each sector) were used to produce each kriging prediction. Table 2.3 provides more detailed information for search neighborhood parameters by stratum.

Table 2.3. Search neighborhood parameters by depth stratum.

DEPTH STRATUM (m)	MINIMUM SEARCH RADIUS (km)	MAXIMUM SEARCH RADIUS (km)	SEARCH ELLIPSOID ANGLE (°)*
0-30	3.353	2.0	64.86
30-100	5.317	2.0	45.00
100-200	12.117	3.0	171.74
200-2,000	6.929	5.0	119.88

*Clockwise from North

At each grid location for which sufficient data existed to produce a kriging prediction, the LOESS trend surface was evaluated and estimates of LOESS prediction standard error and condition number were produced. The kriging prediction, kriging variance, LOESS prediction, LOESS variance, and LOESS condition number were exported from Matlab and GSLIB formats to ESRI GRID format for post-processing using the Spatial Analyst extension in ArcGIS 10 (ESRI, 2011).

The model surface representing predicted depth for each stratum was then calculated as the sum of the LOESS and kriging prediction surfaces (see Equation 2.1). The corresponding prediction variance surface was calculated as the square root of the sum of the LOESS variance and kriging variance estimates. This calculation of the total variance assumes that the spatially structured random error component (δ and ε in Equation 2.1) is uncorrelated with the mean component (μ). The prediction variance was used to construct ±1 standard error and 95% confidence interval surfaces (using the standard normal distribution critical value of 1.96).

Prediction, ±1 standard error, and 95% confidence interval surfaces were back-transformed using the equation:

$$(\text{Exp}(Z_{transform}) - a) / b \qquad \text{(Equation 2.3)}$$

where $Z_{transform}$ is the depth prediction in transformed units and a and b are the error model parameters described for Equation 2.2.

Finally, the separate surfaces representing predicted depth and uncertainty for all four strata were mosaicked to generate seamless surfaces covering the whole study area. At locations with more than one prediction (i.e., where strata overlap), values for the mean (or variance) were calculated by a weighted average, where weights corresponded to the inverse of prediction variance (normalized by the sum of the weights for all the depth strata).

2.3.4 Model Validation and Accuracy Assessment

Cross-validation

A cross-validation exercise was carried out for each depth stratum to assess the accuracy of the geostatistical modeling approach. For purposes of this exercise, 50% of the data points in each stratum were selected at random for inclusion as "training data", with the remaining points held out as "validation data." Models were developed following the methods above applied only to the training data, and predictions were evaluated at the validation data locations. The values of the mosaicked prediction and final mosaicked prediction ± 1 standard error surfaces built from the training dataset were extracted at the validation point locations and cross-validation error statistics (Mean Average Error [MAE], Mean Average Percentage Error [MAPE], and Root Mean Square Error [RMSE]) were calculated. Since the final model was produced using the entire dataset, two times larger than the training dataset, these cross-validation statistics represent a conservative upper bound on the error statistics of the final model.

Independent Accuracy Assessment

In addition to cross-validation, geostatistical model predictions were also compared to depth predictions of the CRM (described in Section 2.1) and to a multibeam dataset, hereafter referred to as the STRATAFORM survey. The STRATAFORM survey collected soundings offshore of New York and New Jersey around 39° 12'N 72°50'W as part of the STRATAFORM project using an EM1000 MBES (Mayer et al., 1999; Nittrouer, 1999; Goff et al., 1999). The STRATAFORM survey covered 2,500 km^2 of seafloor in water depths ranging from 20 to 400 m and provides depth estimates for a contiguous surface at 10 m gridded resolution. Although MBES data does contain some error, for our purposes we consider it to represent the "ground truth" since accuracy and resolution of MBES surveys is much better than interpolated and compiled archival hydrographic surveys. To facilitate comparison, our 83.8 m model grid was overlaid on the 10 m STRATAFORM grid and the mean STRATAFORM values in each model grid cell were calculated. The geostatistical model and CRM, were compared to the STRATAFORM survey within the STRATAFORM survey footprint by calculating mean difference (bias), MAE, MAPE and RMSE. Comparison statistics were calculated for the entire area of overlap and for depth strata within that area (30-100 m, 100-200 m).

2.4 RESULTS AND DISCUSSION

2.4.1 Bathymetry Model Predictions

The new bathymetric model extends over the continental shelf and across the shelf slope, covering the majority of the planning area (Figure 2.5). Depth predictions ranged from 0 m at the shore to around 2,100 m on the shelf slope. Some nearshore areas, like the approach to New York Harbor, were not modeled due to processing limitations arising from extremely high data density. A few small patches in the nearshore areas off southern New Jersey and western Long Island did not have model predictions because the geostatistical model was unable to produce predictions where soundings with distinctly different measured depths occurred at virtually the same location. This occurred where older, less accurate surveys coincided with more recent, more accurate surveys.

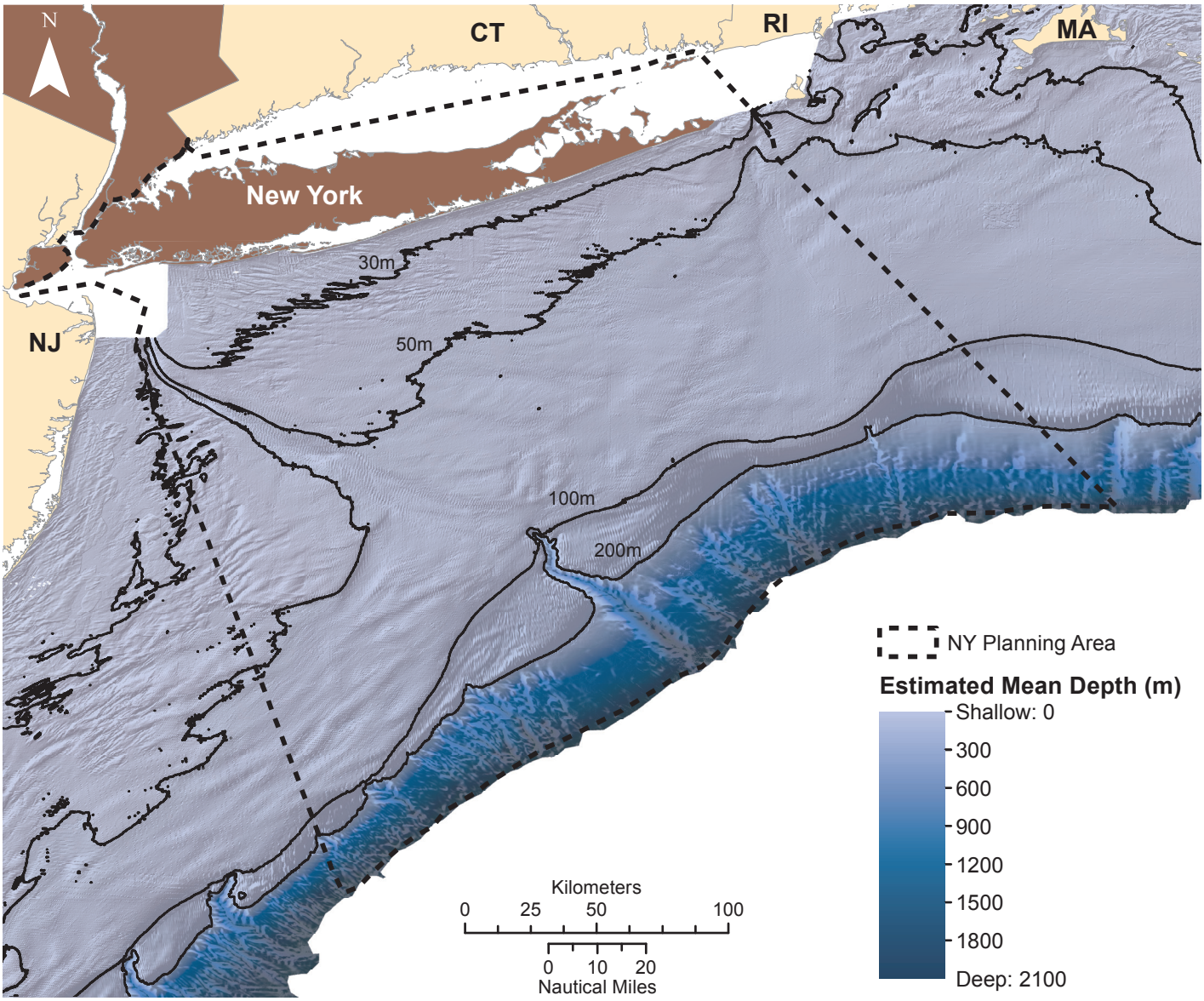

Figure 2.5. Bathymetric surface developed from the geostatistical model, draped over separate hillshade layers derived for the continental shelf (0-200 m) and the shelf slope (>200 m). Solid black lines depict depth contours derived from the bathymetric surface.

Duane et al. (1972) found that sand ridges were a dominant geomorphologic feature on most of the northeast U.S. Atlantic continental shelf. These features were evident in the bathymetry model, particularly to the west of Hudson Canyon and in the northeast of the study area. Submarine canyons, like Hudson Canyon, and shallower networks of gullies were also evident in the model along the shelf slope.

2.4.2 Bathymetry Model Uncertainty

Model standard error ranged from 0.026 m to almost 200 m over the study area (Figure 2.6). In general, model standard error was less than 5 m at depths shallower than 30 m. In this depth stratum, standard error was relatively higher (2-10 m) in areas where surveys occurred prior to 1958 (Figure 2.2). At depths from 30 m to 100 m, standard error was typically less than 2 m, but reached as much as 5 m in some areas where depths approached 100 m. Standard error typically ranged from 2-5 m for depths between 100 and 200 m but was higher (5-10 m) in some areas where depths approached 200 m at the shelf edge. Along the shelf slope, standard error increased from 10-20 m at depths closer to 200 m to greater than 50 m in areas deeper than 500 m. Although standard error generally increased with sounding depth beyond the 30 m depth contour, error was also dependent on distance between surveys. As expected, within each depth stratum, error was generally lower along survey transects where distance between soundings was shortest (lines clearly

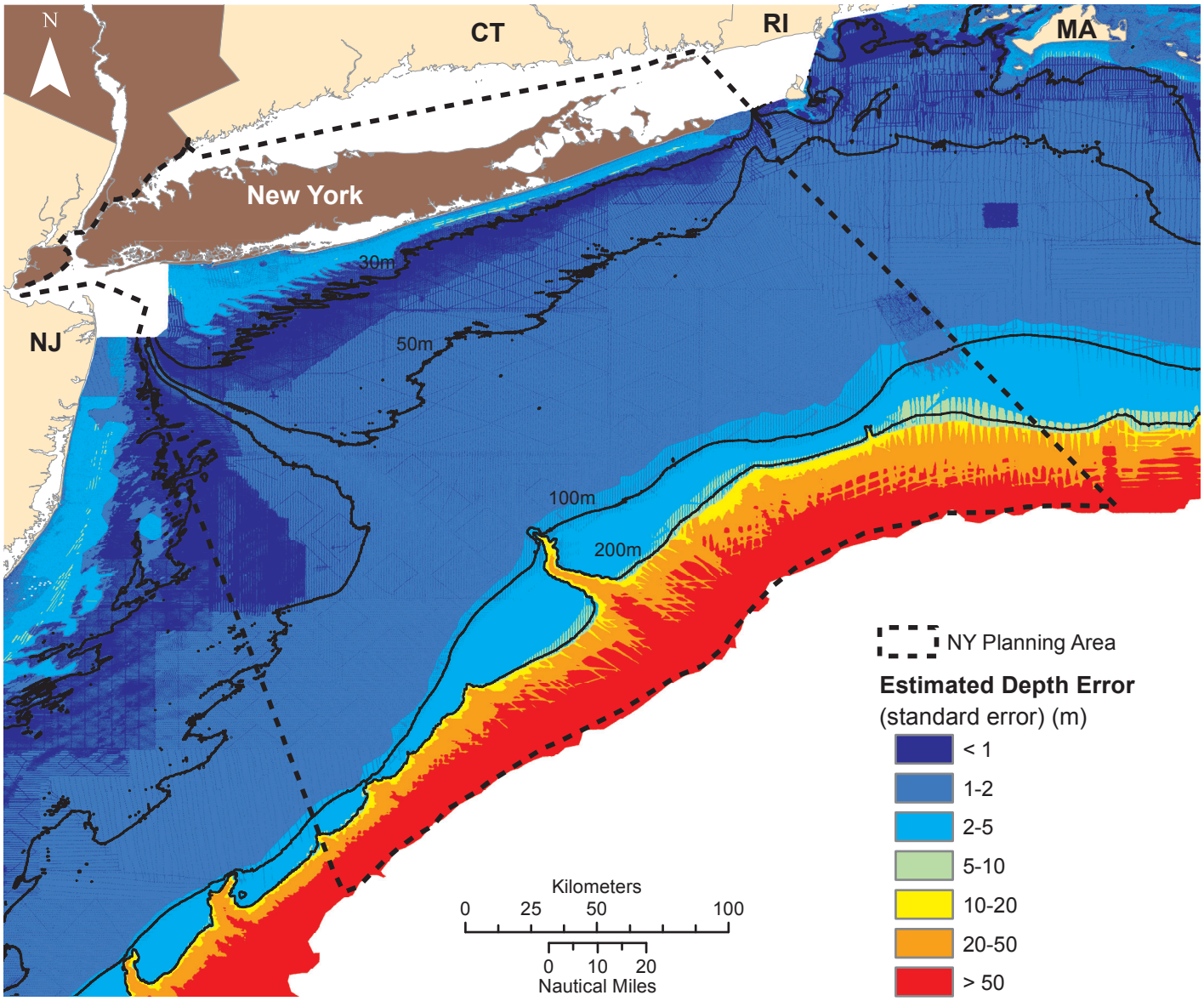

Figure 2.6. Estimated error of predictions (standard error) from the bathymetric model. Model standard error provides an indication of prediction uncertainty.

distinguishable in Figure 2.6). There were two primary reasons for higher error along the shelf slope when compared to shallow areas. First, the absolute precision of sounding instruments generally decreases with depth, and second, soundings become sparser farther offshore. There were several areas south of Hudson Canyon where sounding tracks are greater than 8 kilometers apart (Figure 2.2).

The prediction standard error surface indicates the uncertainty associated with the model prediction at each location, assuming that statistical assumptions of the model are met. Local regressions can be inaccurate as the limits of matrix precision are approached, as indicated by high condition numbers (Figure 2.7). The condition number is a diagnostic that indicates the stability of the local regression trend model at each location. Higher spatial condition number values indicate that the regression solution is less stable at that location, such that small variations in the input data (e.g., uncertainty due to measurement error) can result in large variations in the prediction. For second order polynomials, the critical spatial condition number threshold value is approximately 100, meaning that predictions should be considered with caution at locations where the spatial condition number is close to 100 and should be considered unreliable where it is greater than 100 (Golub and Van Loan, 1996). Under these conditions, the standard error surface may underestimate actual error. This occurs only in a narrow band along the southern coast of Long Island.

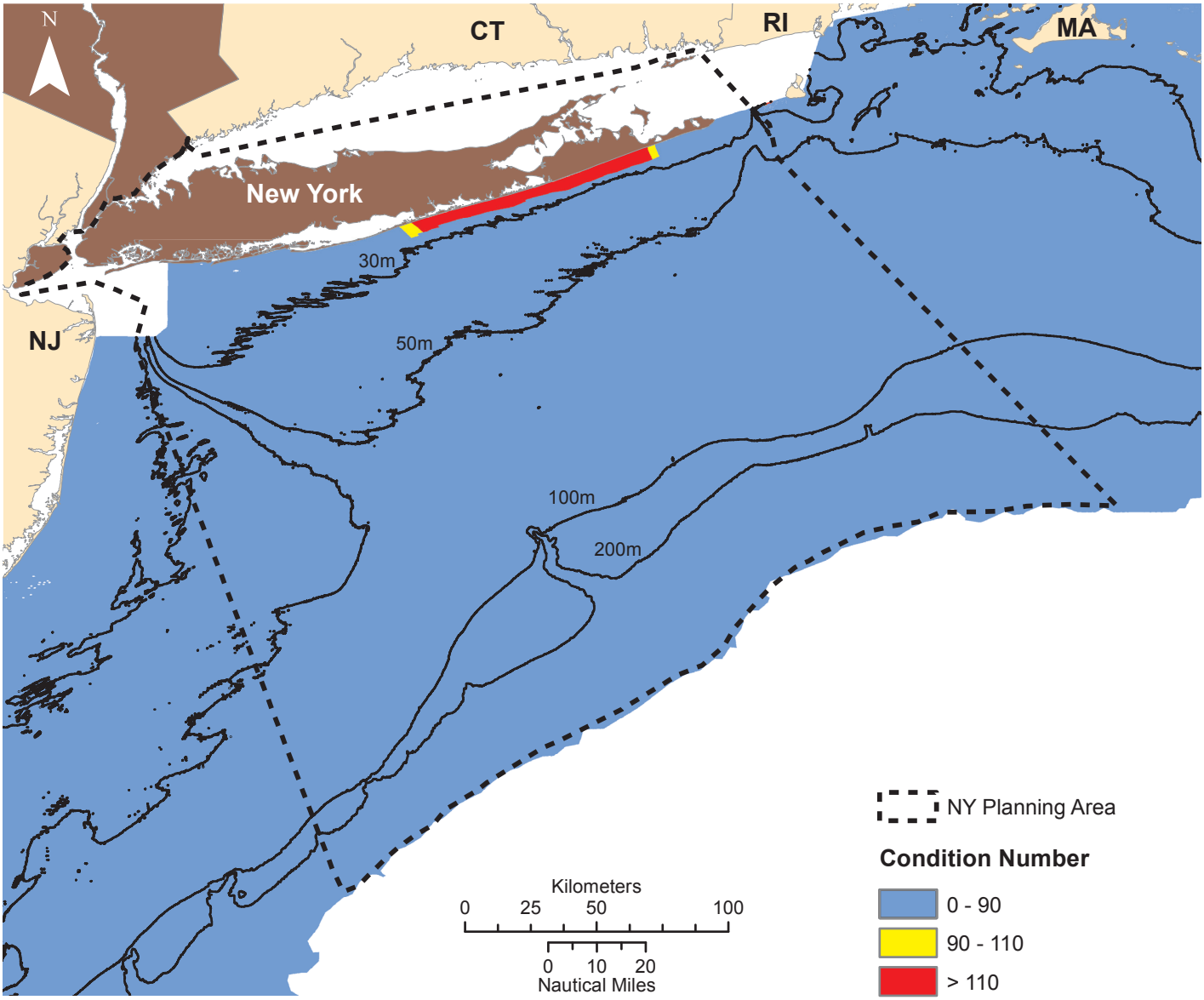

Figure 2.7. Spatial condition number from the LOESS trend model. Condition number classes reflect the threshold at which standard error predictions should be considered unreliable.

Model uncertainty was also depicted using theoretical 95% confidence intervals of the depth predictions (predicted depth ± 1.96*standard error) along two hypothetical transects (Transect 1 and Transect 2) that spanned from the shoreline to the shelf slope (Figure 2.8). Transect 2 differed from Transect 1 in that it cut across a submarine canyon (Hudson Canyon) at the shelf edge. Maximum and minimum depth values representing the upper and lower bounds of the 95% confidence intervals were extracted at 100 m intervals along each transect. For both transects, the width of the 95% confidence intervals generally increased with distance from shore and with depth. However, model uncertainty was greater and more variable in the 0-30 m depth stratum than it was in the 30-100 m depth stratum (Figure 2.9, Figure 2.10). At depths greater than 200 m, the 95% confidence interval widths increased dramatically with distance from shore and had an average vertical width of almost 0.25 km.

To explore how uncertainty in depth predictions may translate into horizontal uncertainty and how this uncertainty could impact management decisions (e.g., the siting of a wind farm), depth contours (30 m, 50 m, 100 m, 200 m) derived from the model prediction and from the upper and lower limits of the theoretical 95% confidence intervals (±1.96*standard error) were overlaid on the boundaries of theoretical wind farm areas within the NY study area (Figure 2.11). These theoretical wind farm areas correspond to areas outside of shipping lanes and within current depth constraints for wind farm structures. These depth contours were mapped to produce a rough estimate of the horizontal uncertainty associated with the model predictions. Within the potential

wind farm areas, transects were drawn between the 50 m depth contours derived from confidence interval limits. The transects were drawn approximately perpendicular to the 50 m depth contour derived from the model prediction at intervals of approximately 5 km.

In this region, the mean distance between the depth contours derived from the confidence interval limits was approximately 8 km with a standard deviation of almost 3 km. While this measure only represents a rough estimate of horizontal uncertainty, it suggests that depth predictions from this model and other models developed using similar data should be used with caution when high positional precision is needed.

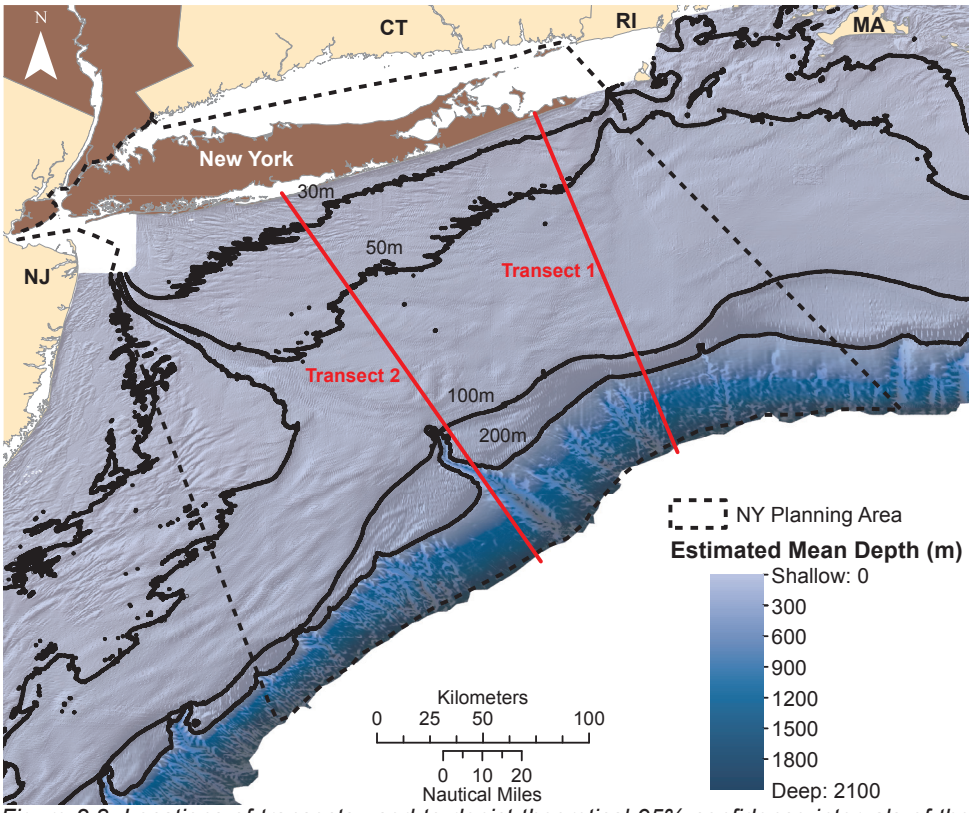

Figure 2.8. Locations of transects used to depict theoretical 95% confidence intervals of the geostatistical model predictions as a function of distance from score and local geomorphology.

2.4.3 Cross-validation of the Training Dataset

Cross-validation results indicated that the geostatistical model performed extremely well in the 0-30 m and 30-100 m depth strata (mean absolute errors 0.60 m and 0.55 m, respectively). The model performed reasonably well in the 100-200 m depth stratum (mean absolute error of 2.1 m, or 1.40%), but model accuracy was considerably degraded in the 200-2,000 m depth stratum (mean absolute error 25.76 m, or 3.44%) (Table 2.4).

Cross-validation was also used to assess the accuracy of confidence intervals. The theoretical 68% confidence intervals (model prediction ± standard error) are somewhat conservative for all depth strata (Table 2.5). For depths below 100 m, the theoretical 95% confidence intervals (model prediction ± 1.96*standard error) are slightly conservative, but the geostatistical model underestimates error at depths greater than 100 m, especially at depths greater than 200 m. For example, in the 200-2,000 m depth range model standard errors should be multiplied by a factor of 2.46, rather than the theoretical value of 1.96, to produce true 95% confidence intervals (Table 2.5).

Table 2.4. Cross-validation statistics for the geostatistical model built from the training dataset. Negative bias indicates a deep bias while positive bias indicates a shallow bias. MAE = Mean Absolute Error, MAPE = Mean Absolute Percentage Error, RMSE = Root Mean Square Error.

DEPTH STRATUM	COMPARISON STATISTIC	CROSS-VALIDATION ERROR
Overall (0-2,000 m)	Bias	-0.08 m
	MAE	1.04 m
	MAPE	6.53%
	RMSE	5.53 m
0-30 m	Bias	-0.17 m
	MAE	0.60 m
	MAPE	7.72%
	RMSE	1.24 m
30-100 m	Bias	0.02 m
	MAE	0.55 m
	MAPE	1.42%
	RMSE	0.96 m
100-200 m	Bias	0.06 m
	MAE	2.14 m
	MAPE	1.40%
	RMSE	5.48 m
200-2,000 m	Bias	2.97 m
	MAE	25.76 m
	MAPE	3.44%
	RMSE	41.23 m

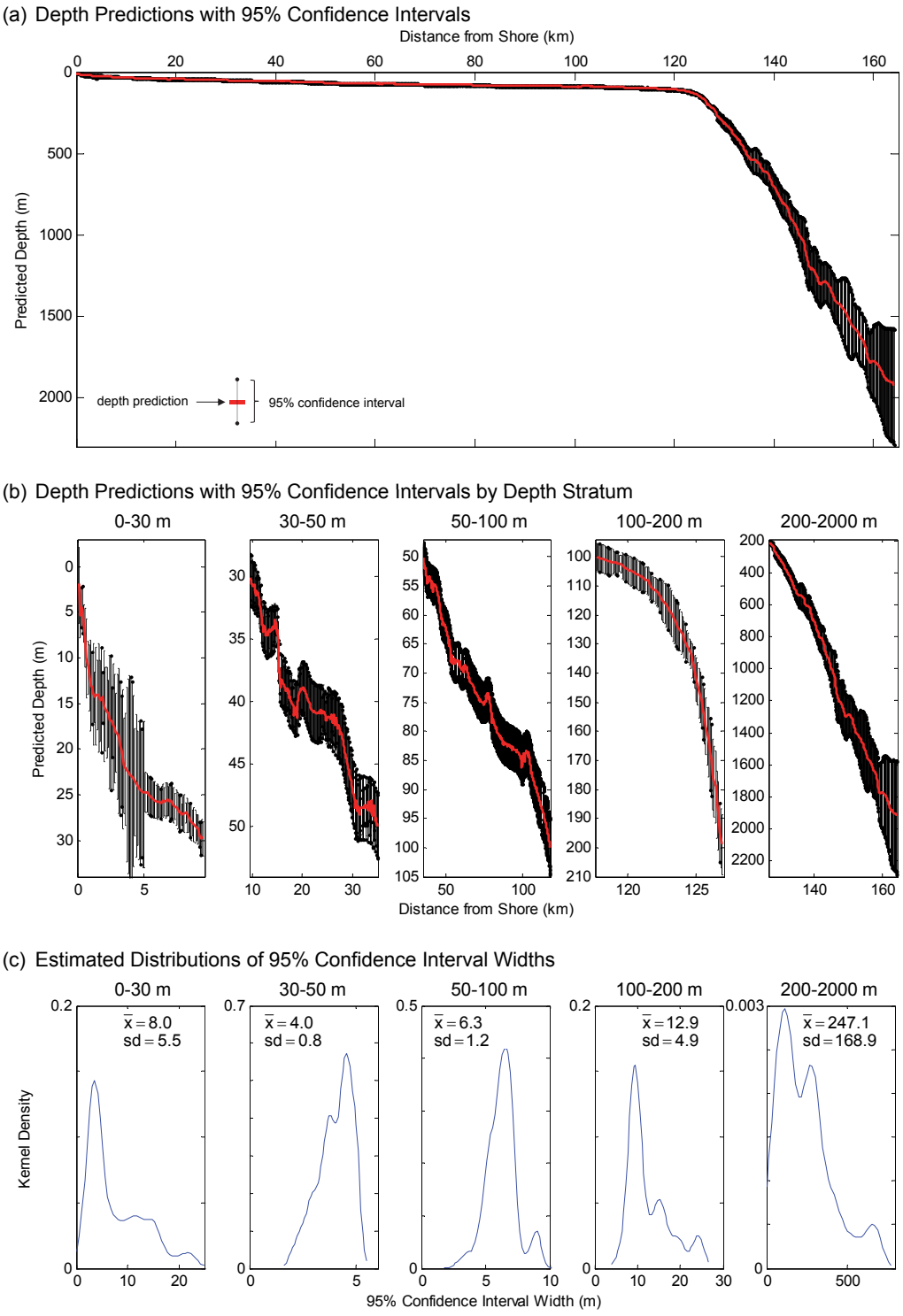

*Figure 2.9. (a) Predicted depth (m) with theoretical 95% confidence intervals (± 1.96*standard error) vs. distance from shore (km) along Transect 1. (b) Predicted depth (m) with 95% confidence intervals by depth stratum. (c) Distribution of 95% confidence interval widths with the mean ($\bar{x}$) and standard deviation (sd) for each depth stratum. The probability density of the confidence interval widths was estimated using a kernel density function (Särkkä 1999).*

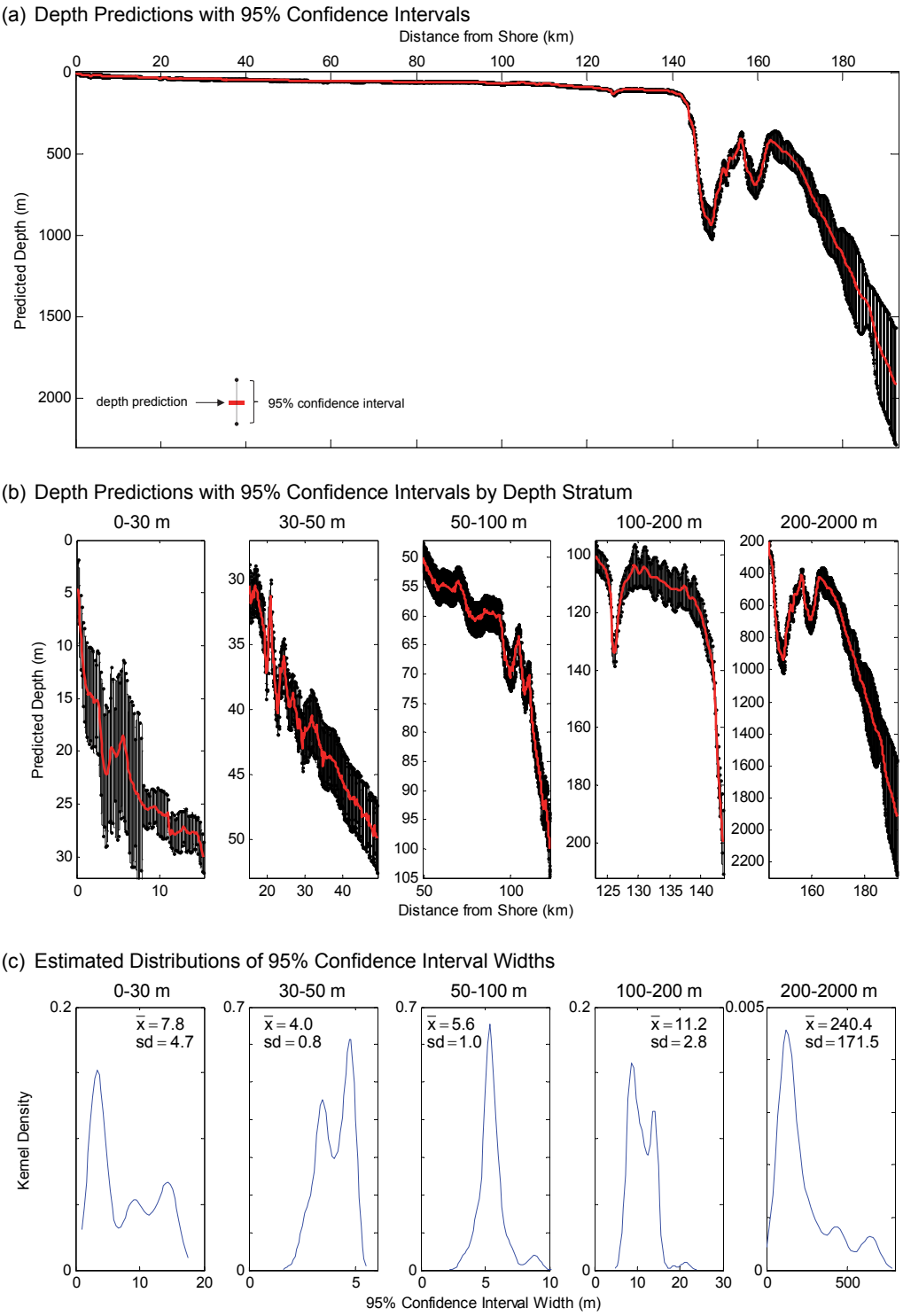

*Figure 2.10. (a) Predicted depth (m) with theoretical 95% confidence intervals (± 1.96*standard error) vs. distance from shore (km) along Transect 2. (b) Predicted depth (m) with 95% confidence intervals by depth stratum. (c) Distribution of 95% confidence interval widths with the mean ($\bar{x}$) and standard deviation (sd) for each depth stratum. The probability density of the confidence interval widths was estimated using a kernel density function (Särkkä 1999).*

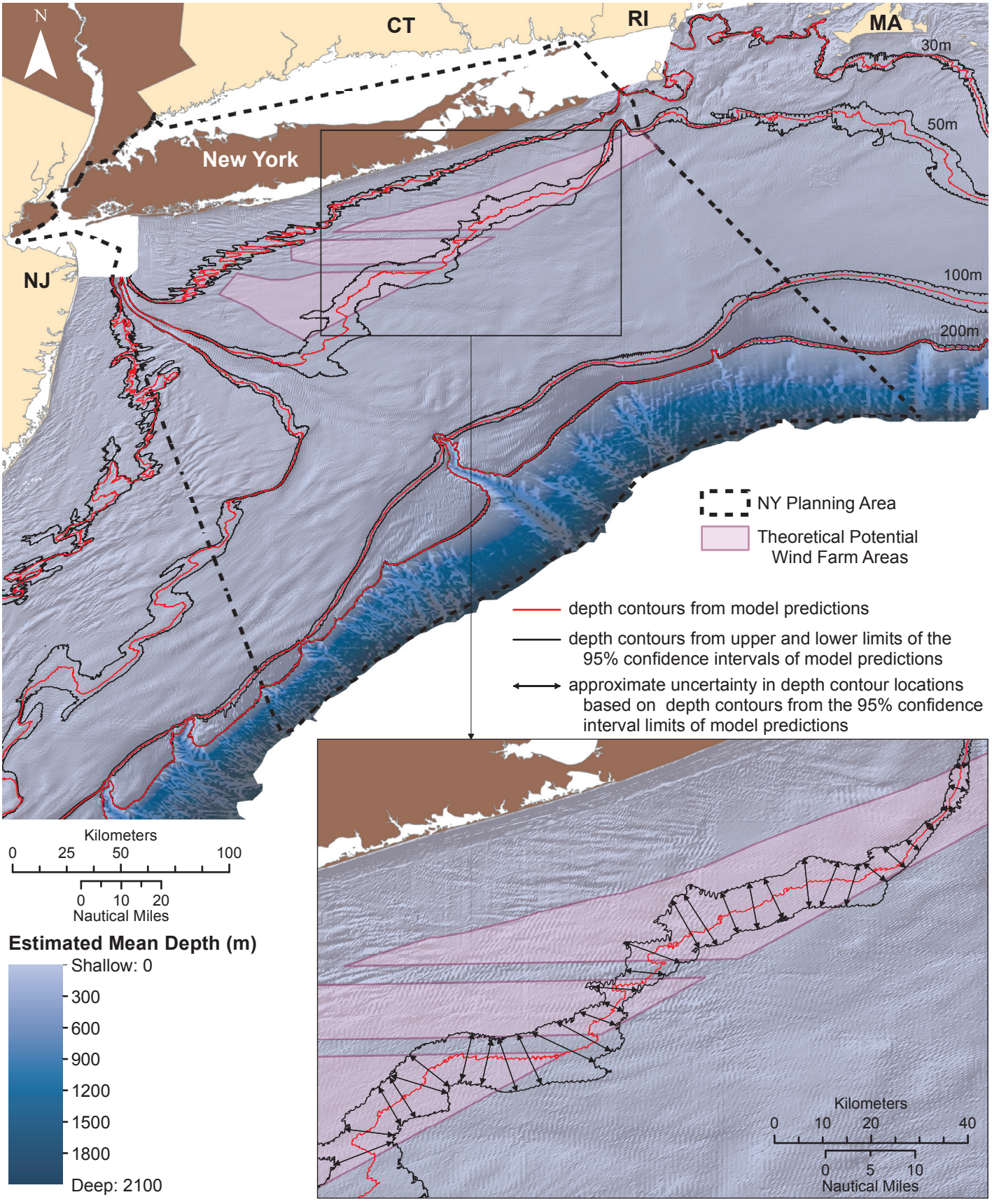

*Figure 2.11. Depth contours derived from the predicted bathymetric surface and from the upper and lower limits of the theoretical 95% confidence intervals (±1.96*standard error) overlaid on the predicted bathymetric surface and theoretical potential wind farm areas for New York. Within the inset map, approximate uncertainty in depth contour locations was estimated using transects approximately perpendicular to the depth contour derived from the predicted bathymetric surface.*

Table 2.5. Performance of theoretical 68% and 95% confidence intervals.

DEPTH STRATUM	PERCENTAGE OF VALIDATION DATA WITHIN THEORETICAL 68% CONFIDENCE INTERVAL	STANDARD ERROR MULTIPLIER FOR 68% CONFIDENCE INTERVAL (COMPARED TO 1.0)	PERCENTAGE OF VALIDATION DATA WITHIN THEORETICAL 95% CONFIDENCE INTERVAL	STANDARD ERROR MULTIPLIER FOR 68% CONFIDENCE INTERVAL (COMPARED TO 1.96)
Overall (0-2,000 m)	87.50%	0.42	95.50%	1.84
0-30 m	87.60%	0.40	95.40%	1.86
30-100 m	87.00%	0.49	95.90%	1.77
100-200 m	88.30%	0.35	94.70%	2.04
200-2,000 m	80.80%	0.62	92.70%	2.46

2.4.4 Independent Accuracy Assessment

The STRATAFORM dataset is ideally located for an independent accuracy assessment of the geostatistical model because it extends across multiple depth strata and overlaps NOS hydrographic soundings collected using multiple sounding and positioning methods.

As a benchmark, we evaluated our model performance in comparison to the CRM in the STRATAFORM area. This may not be an entirely fair comparison, since it is possible (though not verifiable) that the CRM included some version of the STRATAFORM data; however, we proceed anyway with the caution that the CRM error statistics may be significantly better in this region than in other parts of the study area.

Overall we found that both the geostatistical model and CRM are excellent models in the 30-100 m depth range for the STRATAFORM area (mean absolute error [MAE] < 1 m, mean absolute percent error [MAPE] < 1.5%), but accuracy of both models degraded with depth in areas deeper than 100 m (Table 2.6). We found the geostatistical model did not improve upon the CRM in terms of accuracy (when comparing MAE, MAPE, and root mean-square-error [RMSE]) (Table 2.6), but it was able to provide reliable estimates of uncertainty, at least for depths less than 200 m (see Figure 2.6), and obtaining these estimates was the principal reason for undertaking a geostatistical model in the first place. For the 30-100 m and 100-200 m depth strata the percent correct within theoretical 95% confidence intervals were 97.89% and 97.06%, respectively, indicating that the confidence intervals were accurate.

Table 2.6. Results from an accuracy assessment of the geostatistical model and the coastal relief model (CRM). The new geostatistical model and the CRM are compared against the STRATAFORM data. Negative bias indicates a deep bias while positive bias indicates a shallow bias. MAE = Mean Absolute Error, MAPE = Mean Absolute Percentage Error, RMSE = Root Mean Square Error.

DEPTH STRATUM	COMPARISON STATISTIC	INDEPENDENT ACCURACY ASSESSMENT ERROR, GEOSTATISTICAL MODEL	INDEPENDENT ACCURACY ASSESSMENT ERROR, COASTAL RELIEF MODEL
Overall (30-200 m)	Bias	-0.23 m	0.21 m
	MAE	1.17 m	1.15 m
	MAPE	1.18%	1.12%
	RMSE	3.27 m	3.39 m
30-100 m	Bias	0.05 m	0.55 m
	MAE	0.90 m	0.84 m
	MAPE	1.20%	1.10%
	RMSE	1.27 m	1.15 m
100-200 m	Bias	-0.68 m	-0.35 m
	MAE	1.60 m	1.65 m
	MAPE	1.14%	1.15%
	RMSE	5.06 m	5.32 m

Results on bias were mixed. In the 30-100 m depth stratum, the geostatistical model was approximately unbiased, whereas the CRM exhibited a slight shallow bias (+0.55). However, in the 100-200 m depth stratum the geostatistical model exhibited more of a deep bias (-0.68 m) than the CRM (-0.35 m). These biases are small and of the magnitude expected due to known sources of error (e.g., quantization due to rounding of measurement units, changes in tidal references and vertical datums; Calder, 2006).

Taking all comparative data together, the CRM may be the best model if the average value of depth is the primary variable of interest. However, when certainty in depth estimates needs to be accounted for, then the geostatistical model should be preferred, particularly when the depths of interest are shallower than 200 m.

Examples of situations where estimates of bathymetric uncertainty may be useful include measuring the amount of habitat area falling into a given depth range, or identifying suitable construction zones for wind farms based on a depth limit (Figure 2.11). In the latter case, uncertainty can be used to define risk of additional development costs and be used to target the best areas to build within potential construction zones.

2.5 LIMITATIONS TO INTERPRETATION AND FUTURE DIRECTIONS

The geostatistical approach we have employed to create a gridded, interpolated bathymetry surface is an improvement over previous bathymetry models in that it generates a spatially explicit error map to accompany the predicted surface. The cross-validation and independent accuracy assessments show that the model performs similar to the NOAA Coastal Relief Model with the advantage of providing reliable uncertainty estimates. However, several limitations and potential improvements to our approach should be noted here to support interpretation of our models and development of future efforts. Noted limitations will also apply to the CRM and other modeling techniques. Principal limitations of our geostatistical models arise from three general factors:

1) data quality: integrating diverse soundings collected over time and using different methodologies results in a variety of potential distortions in the final surface,
2) resolution: the spatial resolution of original sample data and of the model output grid limit the minimum scale of features that can be resolved, and,
3) model assumptions: geostatistical models involve a number of simplifying assumptions that do not fully capture the complexity of underlying geomorphological patterns.

To help users better understand limitations and appropriate uses of this model, and to guide development of future models, we provide brief explanations and examples of these limitations below and suggest some potential improvements.

2.5.1 Data Quality

Hydrographic soundings in the study area came from a multitude of surveys spanning more than a century (1887-2004). Surveys used an assortment of positioning and sounding technologies, resulting in a patchwork of overlapping soundings collected at varying sample spacings and with different precisions. These errors can propagate to the final model creating distortions that do not correspond to changes on the seafloor.

We have not dealt explicitly with horizontal positioning error. The impact of horizontal positioning error will show up in our models as an increase in the nugget effect over the actual instrument measurement error. Some studies have integrated estimates of positioning uncertainty explicitly into spatial models (Kielland and Tubman, 1994; Jakobsson et al., 2002). Kielland and Tubman (1994) used pseudo-points about the nominal location to combine ship position uncertainties with modeling uncertainties. Jakobsson et al. (2002) used a direct simulation Monte Carlo method in which an ensemble of possible data configurations were drawn assuming a distribution of positioning errors. These approaches could be used to improve the precision of our estimates of bathymetric uncertainty by accounting for differences in positioning certainty between older and newer data.

We also did not explicitly account for differences and possible systematic biases in vertical accuracy of survey data. Archival NOS Hydrographic Survey data has been processed using varying methods over the years which have created some systematic post-processing errors (see Calder, 2006 for a full discussion). Briefly, Calder (2006) reported that archival lead line soundings (common prior to 1978) are systematically shallow-biased because of “hydrographic rounding” (a tendency to round down to the next shallowest whole fathom). Generally, the more recent VBES data appears approximately unbiased (but see below), and modern multibeam surveys offer the most precise information. Calder’s findings suggest that some older VBES soundings are also biased

because they were digitized from paper charts for which data were first rounded to the next shallowest foot or fathom (listed in the metadata as “smooth sheets digitized for NOS under contract”). It may be impossible to correct for biases in these data because the precise procedures followed were not recorded. More recent data entered directly into the database after collection by digital instruments are less likely to have systematic rounding error.

For our purposes, we applied a correction factor to lead line surveys because these were found to have a predictable, systematic error in our study area (Calder, 2006). However, we were unable to correct for probable systematic biases in other sounding methods (e.g., VBES data that went through a smooth sheet digitization). Survey metadata indicates that approximately 18% of soundings were non-lead line data that were digitized using smooth sheets, and therefore would be improved by some bias correction. We attempted to reduce the effect of these potentially biased surveys by eliminating data from those surveys where they fell within the footprint of more modern surveys known to be unbiased (direct digitally ingested VBES and MBES). However, unfortunately, about 40% of the study area was only covered by archival lead line data and/or VBES data digitized from paper charts. These areas are less reliable and may contain systematic biases (typically shallow-biased by <2 m) that are not fully reflected in our model uncertainty estimates. In places where only older, less reliable data are available, we suggest using maps of survey age (Figure 2.2) and/or estimated survey measurement error based on the technique used for sounding (Figure 2.12) to supplement model-based uncertainty maps. These maps viewed alongside geostatistical model errors can help identify unreliable areas and areas where additional bathymetric information would improve future planning decisions.

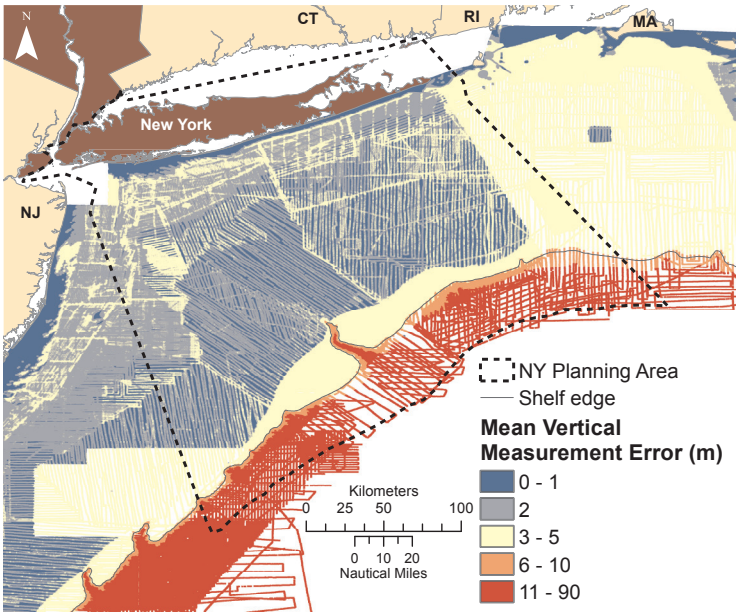

Figure 2.12. Mean estimated vertical measurement error for soundings within 1 km rectangular neighborhoods. Vertical measurement errors were estimated based on vertical sounding technology used. For some surveys this was inferred from survey age. The shelf edge corresponds to the 200 m depth contour.

We have purposefully neglected consideration of changes to the seafloor occurring over time. Temporal changes may or may not be reflected in spatially-explicit model error estimates depending on the ages of nearby surveys. We expect positional error attributed to change over time may be substantial in some areas, especially in highly dynamic areas, such as where tidal and riverine influences are great.

Finally, we note that recently developed geostatistical algorithms could be used in the future to account for heterogeneous measurement error among methods (Christensen, 2011) to improve accuracy and more appropriately weight higher quality data.

2.5.2 Resolution

The distance between soundings was not uniform across the study area (Figure 2.2). The length scale of features that can be resolved will be shorter (higher resolution) in areas with greater sounding density. Moreover, it is possible that our model-based uncertainties will underestimate true error in areas with sparse soundings, especially when very high amplitude, high frequency features are present (e.g., high frequency, short-wavelength sand waves). The chances of this and other problems arising from interactions of sample spacing and high-frequency features (e.g., aliasing) are greater when samples are both sparse and very regularly spaced. Fortunately, in our cross-validation and independent accuracy assessment we did not find evidence for significant overall underestimation of uncertainty, but localized impacts are still possible in areas with high frequency features relative to sample spacing (e.g., sand waves).

In general, fine-scale or very sharply defined features, such as erratics, deep sea reefs or man-made artifacts, will not be reliably resolved in our model. The spatial scale at which these features become visible is dependent on the relative distribution of soundings, the methods used to model spatial structure and the output resolution of maps. Although the sounding density would support resolution approaching 10 m in some limited areas (see Figure 2.2 where sounding density exceeds 100 km^{-1}), the output model grid size was ~85 m. The minimum scale of resolved length scales is twice the output resolution, or ~170 m. For the vast majority of the study area data density was much sparser and could only detect features at scales on the order of 10^2 m and in some areas 10^3 m. In general, new MBES and/or sidescan sonar surveys are needed if greater detectability at short spatial scales is required. In some cases, modern VBES surveys acquired with co-registered sidescan information may be used to identify some missed features. Additionally, Calder (2006) presents a unique method of integrating a variance term corresponding to "hydrographic oversight" of smaller features, but the term requires a very good understanding of the data and geomorphology.

2.5.3. Model Assumptions

A full discussion of the statistical assumptions inherent in the LOESS local regression and geostatistical approaches used here is beyond the scope of this chapter; the reader is referred to texts on the subjects (e.g., Cleveland and Devlin, 1988; Cressie, 1993; Chiles and Delfiner, 1999). However, it is important to note here that geostatistical models are not capable of reproducing the full complexity of geomorphological patterns (e.g., alluvial fans, sand waves) unless data are very dense. This is because geostatistical models describe spatial correlation as a simple function of distance between points, allowing only for very simple geometric anisotropy. Complex multi-point erosional and depositional patterns can't be resolved unless they are densely sampled. Texture-mapping approaches could possibly improve prediction of complex geomorphology (e.g., Boucher, 2009). Ultimately, however, collection of new multibeam bathymetry is preferable to any attempt to statistically reconstruct fine-level details in archival hydrographic surveys.

2.6 ACKNOWLEDGMENTS

We thank Brian Calder and Larry Mayer (The Center for Coastal and Ocean Mapping & NOAA/UNH Joint Hydrographic Center) for providing the gridded STRATAFORM multibeam data used in the accuracy assessment. Bryan Costa, Will Sautter, Tim Battista provided helpful discussions in support of this work and also assisted with data acquisition/analysis for bathymetry and vector shorelines. We are grateful to Brian Calder and John Goff for detailed technical reviews and for discussions that substantially improved this work; however, they are not responsible for any errors or omissions in the final product.

2.7 REFERENCES

Amante, C. and B.W. Eakins. 2009. ETOPO1 1 arc-minute global relief model: procedures, data sources and analysis. NOAA Technical Memorandum NESDIS NGDC-24. 19 pp.

Boucher, A. 2009. Considering complex training images with search tree partitioning. Computers and Geosciences 35:1151-1158.

Butman, B., W.W. Danforth, W.C. Schwab, and M.R. Buchholtz ten Brink. 1998. Multibeambathymetric and backscatter maps of the Upper Hudson Shelf Valley and adjacent shelf, offshore of New York. U. S. Geological Survey Open-File Report 98-616.

Butman, B., T.J. Middleton, E.R. Thieler, and W.C. Schwab. 2003. Topography, shaded relief, and backscatter intensity of the Hudson Shelf Valley, offshore of New York. U. S. Geological Survey Open-File Report 03-372.

Butman, B., D.C. Twichell, P.A. Roma, B.E. Tucholke, T.J. Middleton, and J.M. Robb. 2006. Sea floor topography and backscatter intensity of the Hudson Canyon region offshore of New York and New Jersey. U.S. Geological Survey Open-File Report 2004-1441.

Calder, B.R. 2006. On the uncertainty of archive hydrographic datasets. IEEE Journal of Oceanic Engineering 31(2): 249-265.

Calderbank, B. 2001. Radio positioning accuracies. Lighthouse 59:12-15.

Chiles, J. P. and P. Delfiner. 1999. Geostatististics: modelling spatial uncertainty. New York: Wiley-Interscience.

Christensen, W.F. 2011. Filtered kriging for spatial data with heterogeneous measurement error variances. Biometrics. DOI: 10.1111/j.1541-0420.2011.01563.x.

Cleveland, W.S. and S.J. Devlin. 1988. Locally weighted regression: an approach to regression analysis by local fitting. Journal of the American Statistical Association 83(403):596-610.

Cressie, N.A.C. 1993. Statistics for spatial data (revised ed.). New York: John Wiley & Sons, Inc.

Curry, R.G. 1996. HydroBase: a database of hydrographic stations and tools for climatological analysis. Woods Hole Oceanographic Institution Technical Report WHOI 96-01, 44 pp.

Deutsch, C.V. and A.G. Journel. 1992. GSLIB: Geostatistical Software Library and User's Guide. Oxford University Press. 340 pp.

Duane, D.B., M.E. Field, E.P. Meisburger, D.J.P. Swift, and S.J. Williams. 1972. Linear shoals on the Atlantic Inner Continental Shelf, Florida to Long Island. In: Swift, D.J.P., D.B. Duane, and O.H. Pilkey (eds.). Shelf sediment transport: process and pattern. Stroudsburg, PA: Dowden, Hutchinson and Ross.

Durban, M., C.A. Hackett, and I.D. Currie. 1999. Approximate standard errors in semiparametric models. Biometrics 55(3):699-703.

Environmental Systems Research Institute, Inc. (ESRI). 2011. ArcGIS Desktop: Release 10. Redlands, CA: Environmental Systems Research Institute.

ESRI Online. 2011. ArcGIS Online World Imagery service from ESRI ArcGIS Online and data partners, including imagery from agencies supplied via the Content Sharing Program. Available from http://www.arcgis.com/home/, Accessed Dec 14, 2011.

Gardner, J.V., P. Dartnell, L.A. Mayer, and J.E. Hughes-Clarke. 2003. Geomorphology, acoustic backscatter, and processes in Santa Monica Bay from multibeam mapping. Marine Environmental Research 56:15-46.

Goff, J.A., D.J.P. Swift, C.S. Duncan, L.A. Mayer, and J. Hughes-Clarke. 1999. High resolution swath sonar investigation of sand ridge, dune and ribbon morphology in the offshore environment of the New Jersey Margin. Marine Geology 161:309–339.

Goff, J.A., C.J. Jenkins, and B. Calder. 2006. Maximum likelihood resampling of noisy, spatially correlated data. Geochemistry, Geophysics, and Geosystems 7, Q08003, DOI:10.1029/2006GC001297.

Golub, G.H. and C.F. Van Loan. 1996. Matrix Computations, 3rd edition. Johns Hopkins University Press.

International Hydrographic Organization. 1998. IHO Standards for Hydrographic Surveys, Special Publication No. 44, 4th Edition.

Jakobsson, M., B. Calder, and L. Mayer. 2002. On the effect of random errors in gridded bathymetric compilations. Journal of Geophysical Research – Solid Earth 107(B12).

Kielland, P. and T. Tubman. 1994. On estimating map model errors and GPS position errors: applying more science to the art of navigation. Navigation 41:479-499.

Kostylev, V.E., B.J. Todd, G.B.J. Fader, R.C. Courtney, G.D.M. Cameron, and R.A. Pickrill. 2001. Benthic habitat mapping on the Scotian shelf, based on multibeam bathymetry, surficial geology and sea floor photographs. Marine Ecology Progress Series 219:121-137.

The MathWorks Inc. 2003. MATLAB version 7.13 (R2011b) Natick, Massachusetts.

Mayer, L., L. Fonseca, M. Pacheco, S. Galway, J. Martinez, and T. Hou. 1999. The STRATAFORM GIS, U.S. Office of Naval Research (ONR), St. Andrews, Canada.

Nittrouer, C. STRATAFORM: overview of its design and synthesis of its results. Marine Geology 154(1-4):3-12.

Särkkä, S. 1999. Kernel1 function (for MATLAB). Downloaded November 2011.

Schwab, W.C., W. Corso, M.A. Alison, J.F. Denny, L. Lotto, W.W. Danforth, D.S. Foster, T.F. O'Brien, D.A. Nichols, B.J. Irwin, and K.F. Parolski. 1997a. Mapping the sea floor geology offshore of the New York-New Jersey metropolitan area using sidescan sonar: preliminary report. U.S. Geological Survey Open-File Report 97-61.

Schwab, W.C., M.A. Allison, W. Corso, L.L. Lotto, B. Butman, M. Buchholtz ten Brink, J. Denny, W.W. Danforth, and D.S. Foster. 1997b. Initial results of high-resolution sea-floor mapping offshore of the New York - New Jersey metropolitan area using sidescan sonar. Northeastern Geology and Environmental Sciences 19(4):243-262.

Tagliasacchi, A. 2011. KD-Tree (Library for MATLAB). Downloaded August 2011 from http://www.mathworks.com/matlabcentral/fileexchange/21512-kd-tree-for-matlab.

Tobler, W. 1970. A computer movie simulating urban growth in the Detroit region. Economic Geography 46:234–240.

This page intentionally left blank.